with AML1 and acts as a repressor of AML1-induced transactivation. Biochem. Biophys. Res. Commun. 252:582–589.
14. **Kanno, T., Y. Kanno, L. F. Chen, E. Ogawa, W. Y. Kim, and Y. Ito.** 1998. Intrinsic transcriptional activation-inhibition domains of the polyomavirus enhancer binding protein 2/core binding factor α subunit revealed in the presence of the β subunit. Mol. Cell. Biol. 18:2444–2454.
15. **Kim, W. Y., M. Sieweke, E. Ogawa, H. J. Wee, U. Englmeier, T. Graf, and Y. Ito.** 1999. Mutual activation of Ets-1 and AML1 DNA binding by direct interaction of their autoinhibitory domains. EMBO J. 18:1609–1620.
16. **Kitabayashi, I., A. Yokoyama, K. Shimizu, and M. Ohki.** 1998. Interaction and functional cooperation of the leukemia-associated factors AML1 and p300 in myeloid cell differentiation. EMBO J. 17:2994–3004.
17. **Kitabayashi, I., Y. Aikawa, L. A. Nguyen, A. Yokoyama, and M. Ohki.** 2001. Activation of AML1-mediated transcription by MOZ and inhibition by the MOZ-CBP fusion protein. EMBO J. 20:7184–7196.
18. **Levanon, D., R. E. Goldstein, Y. Bernstein, H. Tang, D. Goldenberg, S. Stifani, Z. Paroush, and Y. Groner.** 1998. Transcriptional repression by AML1 and LEF-1 is mediated by the TLE/Groucho corepressors. Proc. Natl. Acad. Sci. USA 95:11590–11595.
19. **Lutterbach, B., J. J. Westendorf, B. Linggi, S. Isaac, E. Seto, and S. W. Hiebert.** 2000. A mechanism of repression by acute myeloid leukemia-1, the target of multiple chromosomal translocations in acute leukemia. J. Biol. Chem. 275:651–656.
20. **Mukouyama, Y., N. Chiba, T. Hara, H. Okada, Y. Ito, R. Kanamaru, A. Miyajima, M. Satake, and T. Watanabe.** 2000. The AML1 transcription factor functions to develop and maintain hematogenic precursor cells in the embryonic aorta-gonad-mesonephros region. Dev. Biol. 220:27–36.
21. **Nagata, T., V. Gupta, D. Sorce, W. Y. Kim, A. Sali, B. T. Chait, K. Shigesada, Y. Ito, and M. H. Werner.** 1999. Immunoglobulin motif DNA recognition and heterodimerization of the PEBP2/CBF Runt domain. Nat. Struct. Biol. 6:615–619.
22. **Niki, M., H. Okada, H. Takano, J. Kuno, K. Tani, H. Hibino, S. Asano, Y. Ito, M. Satake, and T. Noda.** 1997. Hematopoiesis in the fetal liver is impaired by targeted mutagenesis of a gene encoding a non-DNA binding subunit of the transcription factor, polyomavirus enhancer binding protein 2/core binding factor. Proc. Natl. Acad. Sci. USA 94:5697–5702.
23. **North, T., T. L. Gu, T. Stacy, Q. Wang, L. Howard, M. Binder, M. Marin-Padilla, and N. A. Speck.** 1999. Cbfa2 is required for the formation of intra-aortic hematopoietic clusters. Development 126:2563–2575.
24. **Okada, H., T. Watanabe, M. Niki, H. Takano, N. Chiba, N. Yanai, K. Tani, H. Hibino, S. Asano, M. L. Mucenski, Y. Ito, T. Noda, and M. Satake.** 1998. AML1(−/−) embryos do not express certain hematopoiesis-related gene transcripts including those of the PU.1 gene. Oncogene 17:2287–2293.
25. **Okuda, T., J. van Deursen, S. W. Hiebert, G. Grosveld, and J. R. Downing.** 1996. AML1, the target of multiple chromosomal translocations in human leukemia, is essential for normal fetal liver hematopoiesis. Cell 84:321–330.
26. **Ozanne, D. M., M. E. Brady, S. Cook, L. Gaughan, D. E. Neal, and C. N. Robson.** 2000. Androgen receptor nuclear translocation is facilitated by the F-actin cross-linking protein filamin. Mol. Endocrinol. 14:1618–1626.
27. **Sasaki, A., Y. Masuda, Y. Ohta, K. Ikeda, and K. Watanabe.** 2001. Filamin A associates with Smads and regulates transforming growth factor-β signaling. J. Biol. Chem. 276:17871–17877.
28. **Sasaki, K., H. Yagi, R. T. Bronson, T. K. Tominaga, T. Matsunashi, K. Deguchi, Y. Tani, T. Kishimoto, and T. Komori.** 1996. Absence of fetal liver hematopoiesis in mice deficient in transcriptional coactivator core binding factor β. Proc. Natl. Acad. Sci. USA 93:12359–12363.
29. **Stossel, T. P., J. Condeelis, L. Cooley, J. H. Hartwig, A. Noegel, M. Schleicher, and S. S. Shapiro.** 2001. Filamins as integrators of cell mechanics and signalling. Nat. Rev. Mol. Cell Biol. 2:138–145.
30. **Tahirov, T. H., T. Inoue-Bungo, H. Morii, A. Fujikawa, M. Sasaki, K. Kimura, M. Shiina, K. Sato, T. Kumasaka, M. Yamamoto, S. Ishii, and K. Ogata.** 2001. Structural analyses of DNA recognition by the AML1/Runx-1 Runt domain and its allosteric control by CBFβ. Cell 104:755–767.
31. **Tanaka, K., T. Tanaka, M. Kurokawa, Y. Imai, S. Ogawa, K. Mitani, Y. Yazaki, and H. Hirai.** 1998. The AML1/ETO(MTG8) and AML1/Evi-1 leukemia-associated chimeric oncoproteins accumulate PEBP2β (CBFβ) in the nucleus more efficiently than wild-type AML1. Blood 91:1688–1699.
32. **Tanaka, Y., T. Watanabe, N. Chiba, M. Niki, Y. Kuroiwa, T. Nishihira, S. Satomi, Y. Ito, and M. Satake.** 1997. The protooncogene product, PEBP2β/CBFβ, is mainly located in the cytoplasm and has an affinity with cytoskeletal structures. Oncogene 15:677–683.
33. **Tanaka, Y., M. Fujii, K. Hayashi, N. Chiba, T. Akaishi, R. Shineha, T. Nishihira, S. Satomi, Y. Ito, T. Watanabe, and M. Satake.** 1998. The chimeric protein, PEBP2β/CBFβ-SMMHC, disorganizes cytoplasmic stress fibers and inhibits transcriptional activation. Oncogene 17:699–708.
34. **Wang, Q., T. Stacy, M. Binder, M. Marin-Padilla, A. H. Sharpe, and N. A. Speck.** 1996. Disruption of the Cbfa2 gene causes necrosis and hemorrhaging in the central nervous system and blocks definitive hematopoiesis. Proc. Natl. Acad. Sci. USA 93:3444–3449.
35. **Wang, Q., T. Stacy, J. D. Miller, A. F. Lewis, T. L. Gu, X. Huang, J. H. Bushweller, J. C. Bories, F. W. Alt, G. Ryan, P. P. Liu, A. Wynshaw-Boris, M. Binder, M. Marin-Padilla, A. H. Sharpe, and N. A. Speck.** 1996. The CBFβ subunit is essential for CBFα2 (AML1) function in vivo. Cell 87:697–708.
36. **Warren, A. J., J. Bravo, R. L. Williams, and T. H. Rabbitts.** 2000. Structural basis for the heterodimeric interaction between the acute leukaemia-associated transcription factors AML1 and CBFβ. EMBO J. 19:3004–3015.
37. **Yagi, R., L. F. Chen, K. Shigesada, Y. Murakami, and Y. Ito.** 1999. A WW domain-containing yes-associated protein (YAP) is a novel transcriptional co-activator. EMBO J. 18:2551–2562.
38. **Zaidi, S. K., A. J. Sullivan, R. Medina, Y. Ito, Y. J. Van Wijnen, J. L. Stein, J. B. Lian and G. S. Stein.** 2004. Tyrosine phosphorylation controls Runx2-mediated subnuclear targeting of YAP to repress transcription. EMBO J. 23:790–799.
39. **Zhang, D. E., C. J. Hetherington, S. Meyers, K. L. Rhoades, C. J. Larson, H. M. Chen, S. W. Hiebert, and D. G. Tenen.** 1996. CCAAT enhancer-binding protein (C/EBP) and AML1 (CBF α2) synergistically activate the macrophage colony-stimulating factor receptor promoter. Mol. Cell. Biol. 16:1231–1240.

Overexpression of the Runx3 Transcription Factor Increases the Proportion of Mature Thymocytes of the CD8 Single-Positive Lineage[1]

Kazuyoshi Kohu,* Takehito Sato,[§] Shin-ichiro Ohno,[§] Keitaro Hayashi,* Ryuji Uchino,* Natsumi Abe,* Megumi Nakazato,* Naomi Yoshida,* Toshiaki Kikuchi,[†] Yoichiro Iwakura,[¶] Yoshihiro Inoue,[‡] Toshio Watanabe,* Sonoko Habu,[§] and Masanobu Satake[2]*

The Runx family of transcription factors is thought to regulate the differentiation of thymocytes. Runx3 protein is detected mainly in the $CD4^-8^+$ subset of T lymphocytes. In the thymus of *Runx3*-deficient mice, *CD4* expression is de-repressed and $CD4^-8^+$ thymocytes do not develop. This clearly implicates Runx3 in *CD4* silencing, but does not necessarily prove its role in the differentiation of $CD4^-8^+$ thymocytes per se. In the present study, we created transgenic mice that overexpress *Runx3* and analyzed the development of thymocytes in these animals. In the *Runx3*-transgenic thymus, the number of $CD4^-8^+$ cells was greatly increased, whereas the numbers of $CD4^+8^+$ and $CD4^+8^-$ cells were reduced. The $CD4^-8^+$ transgenic thymocytes contained mature cells with a $TCR^{high}HSA^{low}$ phenotype. These cells were released from the thymus and contributed to the elevated level of $CD4^-8^+$ cells relative to $CD4^+8^-$ cells in the spleen. Runx3 overexpression also increased the number of mature $CD4^-8^+$ thymocytes in mice with class II-restricted, transgenic *TCR* and in mice with a class I-deficient background, both of which are favorable for $CD4^+8^-$ lineage selection. Thus, Runx3 can drive thymocytes to select the $CD4^-8^+$ lineage. This activity is likely to be due to more than a simple silencing of *CD4* gene expression. *The Journal of Immunology,* **2005, 174: 2627–2636.**

Thymocytes pass through multiple, distinct steps of differentiation and gradually develop into immunocompetent T lymphocytes. At each stage of differentiation, thymocytes face fate decisions, such as whether they will survive or die, which lineage they will select, and how they will mature. These events are mostly regulated by a network of signals that are presented to thymocytes as morphogens, cytokines, MHC, and self-Ag peptides (1, 2). The most critical receptors for these signals are the TCR and its coreceptor molecules, CD4 and CD8. Thus, one of the challenging and fascinating steps of thymocyte differentiation is the positive selection of $CD4^+8^+$ double-positive (DP)[3] cells and the subsequent lineage selection to either $CD4^+$ or $CD8^+$ single-positive (SP) cells (3–5). Various transcription factors appear to function coordinately in the regulation of the *TCR*, *CD4*, and *CD8* genes (6, 7).

Recent advances in our understanding of gene regulation in thymocyte differentiation have involved the roles of the Runx family of transcription factors (6). Expression of Runx1 protein is detected in immature, $CD4^-8^-$ double-negative (DN) and premature DP thymocytes, as well as in mature SP thymocytes (8–11). As expected from this expression pattern, Runx1 appears to exert its function at each step of thymocyte differentiation. For example, both the transition of DN cells to the DP stage and the maturation of postselected SP cells are significantly perturbed if the endogenous Runx1 activity in thymus is reduced by artificially expressing a dominant interfering form of Runx1 (8, 11). Each of these steps is normally accompanied by a tremendous amount of cell proliferation, for which Runx1 function is necessary. Conditional targeting of *Runx1* has also revealed that it has an indispensable role in the initial emergence of T-committed cells from stem cells (12).

In contrast to Runx1, the expression of Runx3 protein is detected mainly in the $CD4^-8^+$ subset of thymocytes and splenocytes (9, 10). In accordance with this protein expression profile, $CD4^-8^+$ thymocytes do not develop in the *Runx3* (−/−) thymus (13, 14). Based on an analysis of *CD4* gene regulation, Taniuchi et al. (13) proposed that Runx3 binds to the Runx elements in the *CD4* silencer and represses *CD4* expression. Use of a Morpholino antisense oligonucleotide in an in vitro thymocyte differentiation system also supported the requirement for *Runx3* in the generation of $CD4^-8^+$ cells (10).

These studies clearly implicate Runx3 in the regulation of *CD4* expression, but do not necessarily prove its role in the differentiation of $CD4^-8^+$ thymocytes per se. Loss-of-function experiments provide information about what Runx3 does but not about everything it can do. In the present study, we overexpressed a transgenic Runx3 specifically in the T lineage and analyzed the development of the transgenic thymocytes. Runx3 can actively drive thymocytes to the $CD4^-8^+$ lineage, which implies that it does more than simply silencing *CD4* gene expression.

Departments of *Molecular Immunology, and [†]Oncology and Molecular Medicine, and [‡]Animal Research Facility, Institute of Development, Aging and Cancer, Tohoku University, Sendai, Japan; [§]Department of Immunology, Tokai University School of Medicine, Isehara, Japan; and [¶]Center for Experimental Medicine, Institute of Medical Science, University of Tokyo, Tokyo, Japan

Received for publication April 15, 2004. Accepted for publication November 12, 2004.

The costs of publication of this article were defrayed in part by the payment of page charges. This article must therefore be hereby marked *advertisement* in accordance with 18 U.S.C. Section 1734 solely to indicate this fact.

[1] This work was supported in part by research grants from the Ministry of Education, Science, Sports, Culture and Technology, Japan. M.S. is a member in the 21st century Center of Education program, "Center for Innovative Therapeutic Development Towards the Conquest of Signal Transduction Diseases," which is headed by K. Sugamura at Tohoku University.

[2] Address correspondence and reprint requests to Dr. Masanobu Satake, Department of Molecular Immunology, Institute of Development, Aging and Cancer, Tohoku University, 4-1 Seiryo-machi, Aoba-ku, Sendai 980-8575, Japan. E-mail address: satake@idac.tohoku.ac.jp

[3] Abbreviations used in this paper: DP, double positive; SP, single positive; DN, double negative; HA, hemagglutinin; β_2m, β_2-microglobulin; ISP, immature single positive; E, embryonic day; HSA, heat-stable Ag.

0022-1767/05/$02.00

Materials and Methods

Plasmids

The hemagglutinin (HA) tag that represents the epitope of flu virus HA was fused to the N terminus of the murine Runx3 coding region by the PCR method as follows. PCR was performed using a murine *Runx3* cDNA (15) as a template. The sequences of the sense and antisense primers were 5'-GCC GGA TCC GAA TTC ACC ATG TAT CCA TAT GAT GTT CCA GAT TAT GCT ATG CGT ATT CCC GTA GAC CC-3' and 5'-GCC GGA TCC GAA TTC TTA GTA GGG CCG CCA CAC-3', respectively. The PCR product was digested with *Bam*HI and subcloned into the *Bam*HI site of pLck (p1017), which harbors the proximal promoter region of the murine *Lck* gene and a poly(A) addition sequence derived from the human growth hormone gene (16). The resulting plasmid was designated *pLck-HA/Runx3*. The accuracy of the modified sequences in the plasmid was confirmed by sequencing. Immunohistochemical staining of cDNA-transfected HeLa cells confirmed the nuclear localization of HA-tagged Runx3 protein (data not shown).

Mice

To generate transgenic mouse lines expressing Runx3, the DNA of *pLck-HA/Runx3* was digested with *Spe*I, and the purified fragment containing the Runx3 expression unit was microinjected into fertilized eggs of C57BL/6 mice. Transgenic founders were identified and crossed to C57BL/6 mice. The presence or absence of the transgene was examined by PCR using genomic DNA as a template. The sense and antisense primers were 5'-CGG GAA TTC ATG TAT CCA TAT GAT GTT CCA GAT TAT GCT ATG CGT ATT CCC GTA GAC CC-3' and 5'-CCG GAA TTC TTA GTA GGG CCG CCA CAC-3', respectively, and a 1275-bp fragment was amplified from the transgene. Establishment of the human *CD4*-transgenic mice will be described elsewhere (Y. Iwakura, manuscript in preparation). Briefly, fertilized eggs of C3H/HeN mice were microinjected by the human *CD4* cDNA which harbors the murine *CD4* enhancer/promoter and an *SV40*-derived poly(A) addition signal. *β_2-microglobulin* (*β_2m*)-deficient mice and *CD4*-deficient mice were purchased from The Jackson Laboratory. The I-A^d-restricted, $OVA_{323-339}$-specific TCR-transgenic mice have been previously reported (17).

Flow cytometrical analysis

Cells were liberated from the thymus and spleen and suspended in PBS containing 0.2% (w/v) BSA. The single-cell suspensions were incubated with appropriately diluted mAbs on ice for 30–60 min. The following fluorescein-conjugated mAbs were used: CyChrom-CD4 (Rm4-5), FITC-CD4 (Rm4-5), PE-CD8a (53-6.7), RED613-CD8a (53-6.7; Invitrogen Life Technologies), PE-TCRβ (H57-597), FITC-CD69 (H1.2F3), FITC-Vβ2 (B20.6), FITC-Vβ3 (KJ25), FITC-Vβ4 (KT4), FITC-Vβ5.1 and -5.2, FITC-Vβ6 (RR4-7), FITC-Vβ7 (TR310), FITC-Vβ8.1 and -8.2 (MR5-2), FITC-Vβ8.3 (1B3.3), FITC-Vβ9 (MR10-2), FITC-Vβ10^b (B21.5), FITC-Vβ11 (RR3-15), FITC-Vβ12 (MR11-1), FITC-Vβ13 (MR12-3), FITC-Vβ14 (14-2), FITC-Vβ17^a (KJ23), FITC-HSA (M1-69), and FITC-human CD4 (Leu3a). Except for RED613-CD8a, the mAbs were purchased from BD Pharmingen. The labeled cells were separated with an analytical flow cytometer (EPICS-XL), and the data were analyzed with EXPO32 software (Beckman Coulter).

Immunoblot analysis and EMSA

The $CD4^-8^+HSA^{low}$ and $CD4^+8^-HSA^{low}$ fractions were purified from thymocytes or splenocytes, respectively, using autoMACS (Miltenyi Biotec). Its purity was judged to be >90% by flow cytometry. Protein was extracted from cells using a radioimmunoprecipitation assay solution (50 mM Tris-HCl (pH 7.4), 1% (v/v) Triton X-100, 0.5% (w/v) sodium deoxycholate, 0.1% (w/v) SDS, 150 mM NaCl, 1 μg/ml aprotinin, 1 mM $NaVO_4$, and 1 mM NaF). The other procedures necessary for immunoblot analysis including the electrophoresis, transfer to the filter, and immunoreaction were performed as described previously (18). The raising and characterization of the anti-Runx peptide Ab was also described previously (19). The antiserum raised against the C terminus of murine Runx1 can recognize Runx1, Runx2, and Runx3, because they share the common VWRPY sequence at their extreme C-terminal ends. The anti-tubulin α Ab (Ab-1) was purchased from Oncogene. The procedures for preparing nuclear extracts and for the EMSA were described previously (20). The Runx binding sequence from the *Polyomavirus* enhancer was used as a probe to detect Runx DNA binding activity. The anti-HA mAb 3F10 used for the supershift assay was purchased from Roche Diagnostics.

RT-PCR

Total cytoplasmic RNA was isolated from cells using the ISOGEN reagent (Nippon Gene). cDNAs were synthesized from the RNAs by reverse transcription using Superscript II reverse transcriptase (Invitrogen Life Technologies). The cDNAs were PCR-amplified (25 cycles for each gene) with LA-*Taq* polymerase (Takara), using the following sense and antisense primers to detect transcripts: for *CD4*, 5'-CCT GCG AGA GTT CCC AGA AGA AGA TCA CAG-3' and 5'-TGA TAG CTC TGC TCT GAA AAC CCA GCA CTG-3'; for *CD8α*, 5'-GGT GAG TCG ATT ATC CTG GGG AGT GGA GAA-3' and 5'-ACA CAA TTT TCT CTG AAG GTC TGG GCT TGC-3'; for *perforin1*, 5'-CAA GCA GAA GCA CAA GTT CGT-3' and 5'-CGT GAT AAA GTG CGT GCC ATA-3'; for *GATA3*, 5'-AGG CAA GAT GAG AAA GAG TGC CTC-3' and 5'-CTC GAC TTA CAT CCG AAC CCG GTA-3'; and for *G3PDH*, 5'-ACC ACA GTC CAT GCC ATC AC-3' and 5'-TCC ACC ACC CTG TTG CTG TA-3'. The PCR products were run through agarose gels and visualized with ethidium bromide staining.

Chromatin immunoprecipitation assay

A chromatin fraction was prepared from thymocytes, fixed and immunoprecipitated by the anti-Runx or anti-HA Ab, respectively. The procedures were as recommended by the manufacturer of the assay kit (Upstate Cell Signaling Solutions). DNA was purified from the precipitate and processed as a template for PCR to amplify the *CD4* silencer-specific sequence. The primers for PCR were 5'-TGT AGG CAC CCG AGG CAA AG-3' and 5'-GTT CCA GCA CAG GAG CCC CA-3'. The amplified product was run through agarose gels and transferred to nylon membranes. The membranes were hybridized with ^{32}P-labeled, *CD4* silencer-specific oligonucleotide, 5'-ATA CGA AGC TAG GCA ACA GA-3'.

Results

Overexpression of Runx3 in the T lineage cells

Endogenous expression of Runx3 protein is detected mainly in the $CD4^-8^+$ subset of T lymphocytes (9, 10). To artificially overexpress Runx3 in the T cell lineage, we placed the *Runx3* coding

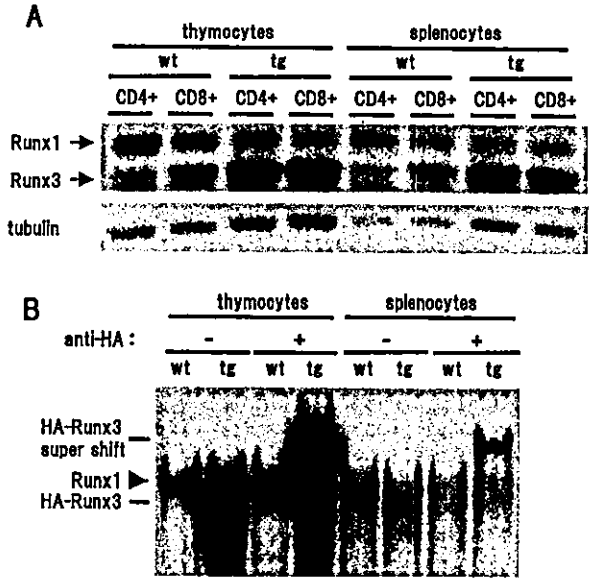

FIGURE 1. Expression of transduced Runx3 protein. *A*, Protein was extracted from thymic and splenic $CD4^+8^-HSA^{low}$ as well as $CD4^-8^+HSA^{low}$ cells and processed for immunoblot analysis. The extracts from wild-type and *Runx3*-transgenic cells were probed with an anti-Runx Ab. The bands indicated by the arrows represent the Runx3 and endogenous Runx1 proteins of 52 and 56 kDa, respectively. An immunoblot with an anti-tubulin α Ab served as a control. *B*, Runx DNA binding activity detected by EMSA. The nuclear extracts from the wild-type and *Runx3*-transgenic thymocytes and splenocytes were processed for EMSA. The bands indicated by the arrowhead and bar represent the activity of endogenous Runx1 and transduced HA-Runx3, respectively. The HA-Runx3-derived band was supershifted by the addition of an anti-HA Ab to the transgenic extract.

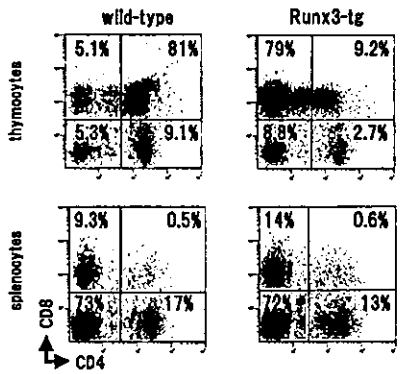

FIGURE 2. Flow cytometrical analysis of thymocytes and splenocytes. The cells from wild-type and *Runx3*-transgenic mice were stained for CD4 and CD8 and processed for flow cytometry. Numbers given in the individual quadrants indicate the percentage of cells of each type.

region under the control of the proximal *Lck* gene promoter. This promoter is known to be active in immature as well as mature T cells and in thymic as well as peripheral T cells (16). Transgenic mouse lines were established and the expression of Runx3 protein was examined by immunoblot analysis using an anti-Runx Ab (Fig. 1*A*). The 52-kDa Runx3 band was clearly detected in the extract of both $CD4^+8^-$ and $CD4^-8^+$ fractions, which were prepared from transgenic thymi as well as spleens. The endogenous Runx3 was also detected in the wild-type, $CD4^-8^+$ thymocytes and splenocytes but to a much lesser degree compared with the transgenic cells. Thus, the magnitude of Runx3 overexpression in the transgenic vs wild-type cells was roughly 5-fold in the case of thymi and 3-fold in the case of spleens. A very faint band seen in the $CD4^+8^-$ wild-type cells represents the nonspecific reaction of the Ab, because the band was not abolished by the preabsorption of the Ab with the Ag peptide. The endogenous Runx1 protein of 56 kDa was detected in all the fractions tested.

We assessed the contribution of overexpressed Runx3 to the Runx-specific DNA binding activity using EMSA (Fig. 1*B*). The endogenous activity detected in a thymocyte extract from wild-type mice was mainly due to the Runx1 protein. The extract from transgenic thymocytes gave rise to a band that migrated slightly faster, reflecting the smaller size of the Runx3 protein compared Runx1 (52 vs 56 kDa). Addition of an anti-HA Ab supershifted the band of the transgenic, HA-tagged Runx3 but not that of the endogenous Runx1 protein. Similar results were seen in the extracts of splenocytes, although the band intensity was much weaker due to the presence of other than the T cells.

The percentage of $CD4^-8^+$ cells increases and the percentage of $CD4^+8^+$ and $CD4^+8^-$ cells simultaneously decreases in the Runx3-transgenic thymus

After confirming the protein expression of transgenic Runx3, we evaluated its effect on T cell differentiation. Flow cytometry was used to analyze CD4 and CD8 in thymocytes and splenocytes (Fig. 2). In the *Runx3*-transgenic thymi, the percentage of $CD4^-8^+$ cells

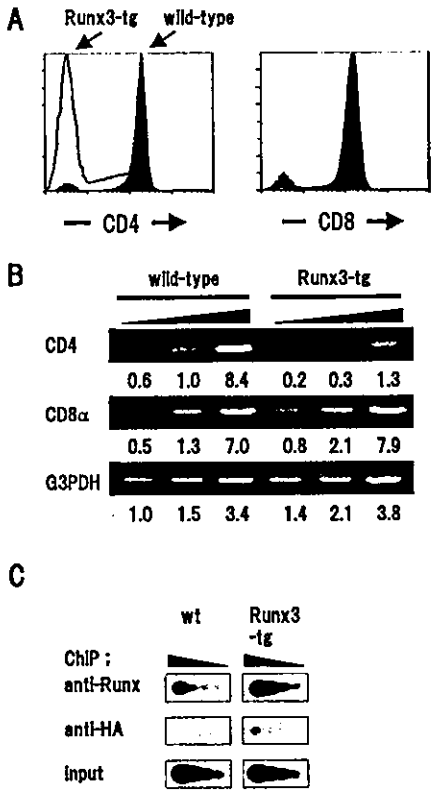

FIGURE 3. CD4 and CD8 expression in the wild-type and *Runx3*-transgenic cells. *A*, Thymocytes stained for CD4 or CD8 were analyzed for their fluorescence intensity. The shaded peak represents the wild-type cells, whereas the open peak represents the *Runx3*-transgenic cells. *B*, Semiquantitative RT-PCR analysis of *CD4*, *CD8α*, and *G3PDH* transcripts. An increasing amount of cDNA synthesized from the wild-type and *Runx3*-transgenic thymocytes was used for PCR. The relative amounts of PCR products were measured and are shown as numbers below the gels. The *G3PDH* product obtained for the least amount of wild-type cDNA was taken to be 1.0. *C*, Chromatin immunoprecipitation analysis. A chromatin fraction prepared from the wild-type and *Runx3*-transgenic thymocytes was immunoprecipitated by an anti-Runx or anti-HA Ab, respectively. DNA was purified from the precipitates, and an increasing amount of DNA fraction was processed as a template for PCR. The PCR products were detected by a *CD4* silencer-specific oligonucleotide. Input means a DNA fraction that was present in the chromatin fraction before immunoprecipitation.

increased to 80% of the total population, whereas the percentage of $CD4^+8^+$ cells decreased to only 9%; the percentage of $CD4^+8^-$ cells also decreased substantially. The unusual profile of CD4 and CD8 expression in the transgenic thymocytes was reflected in the transgenic splenocytes as well. In the transgenic spleen, the percentage of $CD4^-8^+$ cells was higher than that of $CD4^+8^-$ cells, whereas the opposite was true in the wild-type spleen.

We counted the number of cells that were recovered from the thymi and spleens of several individual adult mice (Table I). The number of transgenic thymocytes was ~60% of that of wild-type

Table I. *The numbers and percentages of SP cells in wild-type and Runx3-transgenic thymi and spleens*[a]

	Thymus				Spleen		
	Total cells ($\times 10^8$)	$CD4^+8^+$ (%)	$CD4^+8^-$ (%)	$CD4^-8^+$ (%)	Total cells ($\times 10^8$)	$CD4^+8^-$ (%)	$CD4^-8^+$ (%)
Wild type (n = 9)	2.20 ± 0.67	80.8 ± 1.5	8.73 ± 0.51	5.36 ± 0.63	1.13 ± 0.52	15.5 ± 5.26	7.56 ± 2.38
Runx3-transgenic (n = 9)	1.33 ± 0.46	10.9 ± 1.7	2.21 ± 0.29	78.3 ± 1.7	0.84 ± 0.35	8.73 ± 3.92	10.55 ± 3.85

[a] The means and SD are presented. n, The number of individual mice examined.

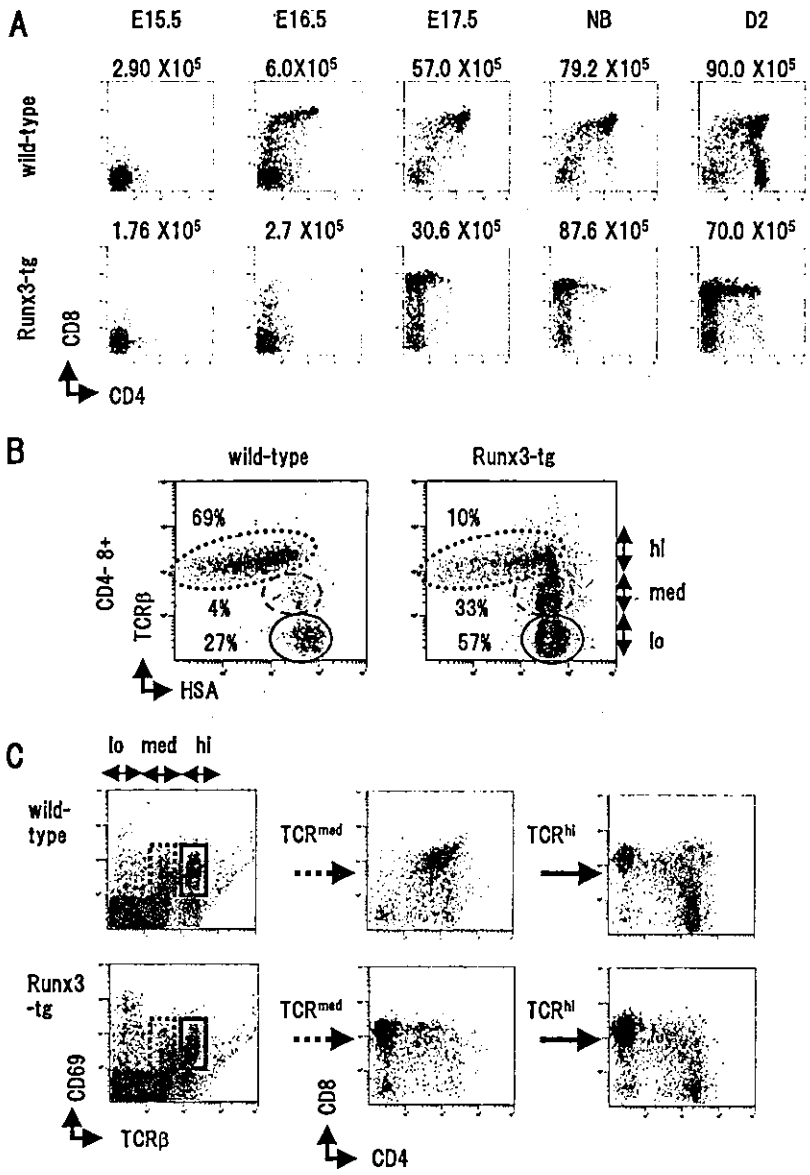

FIGURE 4. Different subpopulations exist in the $CD4^-8^+$ fractions from wild-type and *Runx3*-transgenic thymus. *A*, Ontogeny of thymocyte development. Thymocytes were prepared from wild-type and *Runx3*-transgenic mice at E15.5, E16.5, E17.5, birth (NB), and 2 days after birth (D2). The cells were stained for CD4 and CD8 and processed for flow cytometry. The numbers above each panel indicate the number of cells recovered. *B*, The wild-type and *Runx3*-transgenic thymocytes from adult mice were processed for four-color flow cytometrical analysis. The $CD4^-CD8^+$ fractions were further analyzed for their TCR and HSA expression profiles. The level of TCR expression was classified into three stages (lo, med, and hi), as indicated. The numbers represent the percentages of each subpopulation in the $CD4^-8^+$ fraction. *C*, CD69 and TCR expression profiles in differentiating thymocytes. The wild-type and *Runx3*-transgenic thymocytes were processed for four-color flow cytometry. The cells were first screened for their CD69 and TCR expression profiles. The $TCR^{med}CD69^+$ (broken boxes) and $TCR^{high}CD69^+$ fractions (solid boxes) were further analyzed for their CD4 and CD8 expression profiles.

thymocytes. As a result, the number of cells in the $CD4^-8^+$ fraction was higher, and the number in the $CD4^+8^+$ and $CD4^+8^-$ fractions was lower, in the transgenic thymi compared with the wild-type thymi. The total number of splenocytes did not differ significantly between the two genotypes.

Decrease in the CD4 expression in the Runx3-transgenic thymocytes

The increase in the $CD4^-8^+$ fraction in the *Runx3*-transgenic thymus could be due either to an increase in CD8 expression or a decrease in CD4 expression. To distinguish these two possibilities, the CD8 and CD4 expression profiles were displayed for the wild-type and the *Runx3*-transgenic thymocytes (Fig. 3*A*). The relative ratios of $CD8^-$ and $CD8^+$ cells were not different between the two genotypes. In contrast, the number of $CD4^-$ cells was greatly increased and the number of $CD4^+$ cells was decreased in the transgenic thymus compared with the wild-type thymus.

We also performed a semiquantitative RT-PCR analysis of *CD4* and *CD8* transcripts (Fig. 3*B*). RNA was prepared from the thymocytes, and increasing amounts of the cDNAs were processed for PCR. Although the relative amount of *CD8* transcript did not differ significantly between the two types of cells, many fewer *CD4* transcripts were present in the *Runx3*-transgenic thymocytes compared with the wild-type cells.

The *CD4* silencer is proposed to be a main target by a Runx3 transcription factor (13, 14). We checked this by chromatin immunoprecipitation analysis (Fig. 3*C*). An increasing amount of chromatin fraction-derived DNA that was precipitated by the anti-Runx or anti-HA Ab was processed for PCR and hybridized by a *CD4* silencer-specific oligonucleotide. Both Abs precipitated a significantly greater amount of *CD4* silencer sequence from the *Runx3*-transgenic thymocytes compared with the wild-type cells. The results in Fig. 3 thus suggest that the phenotypic alteration seen in the transgenic thymocytes in Fig. 2 can be at least partly explained by the down-regulation of *CD4* expression.

The increased $CD4^-8^+$ fraction of transgenic thymocytes includes immature, premature, and mature subpopulations

We next characterized in detail the $CD4^-8^+$ fraction of transgenic thymocytes. As described below, this fraction was found to contain three different subpopulations: immature, premature, and mature cells.

The first subpopulation in the $CD4^-8^+$ fraction was recognized as immature single-positive (ISP) cells, which can be easily seen by following the ontogeny of thymocyte development (Fig. 4*A*). In wild-type thymus, only $CD4^-8^-$ cells were detected at embryonic day (E)15.5. $CD4^-8^+$ ISP cells transiently appeared at E16.5, $CD4^+8^+$ cells at E17.5, and $CD4^+8^-$ cells at day 2 after birth. In the *Runx3*-transgenic thymus, immature $CD4^-8^+$ cells first appeared at E16.5 and remained as the main population until after birth. The persistence of ISP cells is probably due to the down-regulation of *CD4* by Runx3. This *CD4* repression appeared to be partial, because some $CD4^+8^+$ and $CD4^+8^-$ cells emerged at day 2 after birth in transgenic mice.

Immature $CD4^-8^+$ cells were also prominent in thymi from adult transgenic mice. To further characterize this population, flow cytometry was first used to select the $CD4^-8^+$ fraction of the thymocytes, and then the expression profiles of TCRβ (hereafter TCR) and heat-stable Ag (HSA) were displayed for this fraction (Fig. 4*B*). The immature $TCR^{low}HSA^{high}$ fraction made up 27% of the wild-type and 57% of the transgenic $CD4^-8^+$ thymocytes. Therefore, overexpression of Runx3 increased the number of ISP cells.

Another characteristic of the transgenic $CD4^-8^+$ fraction was the presence of an aberrant $TCR^{med}HSA^{high}$ subpopulation that was not as apparent in the wild-type fraction (33 vs 4%; Fig. 4*B*). The medium degree of TCR expression indicates that this second subpopulation should be categorized as representing the premature DP stage rather than the ISP stage. We further confirmed this point by staining the thymocytes with CD69, a marker of positive selection (Fig. 4*C*). In the case of wild-type cells, the $TCR^{med}CD69^+$ cells exhibited a $CD4^+8^+$ phenotype, whereas the $TCR^{high}CD69^+$ exhibited both the $CD4^+8^-$ and $CD4^-8^+$ phenotypes. The $TCR^{med}CD69^+$ population could also be detected in the transgenic thymus, but the apparent phenotype of this population was $CD4^-8^+$, not $CD4^+8^+$. The $CD4^-8^+$ fraction persisting in the developing transgenic thymus (Fig. 4*A*) may contain these TCR^{med} cells as well. Thus, the second subpopulation can be summarized as the premature, "CD4-repressed DP" cells.

The transgenic $CD4^-8^+$ fraction also contained a third subpopulation of mature, $TCR^{high}HSA^{low}$ cells (see 10% in Fig. 4*B*). We next evaluated the effect of Runx3 overexpression on these mature $CD4^-8^+$ cells. To do so, we first obtained a TCR expression profile for the total thymocyte population (Fig. 5*A*). Both the wild-type and *Runx3*-transgenic thymi contained TCR^{low}, TCR^{med}, and TCR^{high} subpopulations to a comparable degree. Because the TCR^{high} subpopulation corresponds to mature cells, overexpression of Runx3 did not appear to arrest or block thymocyte differentiation. We gated the TCR^{high} subpopulation and then displayed the CD4/8 profile (Fig. 5*B*). In the TCR^{high} thymocytes from the wild-type, the percentage of $CD4^-8^+$ cells was one-third that of $CD4^+8^-$ cells, whereas in the transgenic TCR^{high} thymocytes, the percentage of $CD4^-8^+$ cells was three times that of $CD4^+8^-$ cells. We also counted the cell numbers constituting each fraction and found that the absolute number of $CD4^-8^+TCR^{high}$ cells in the transgenic thymi was approximately twice that in the wild-type thymi.

To further verify the differentiation stage of the apparently mature $CD4^-8^+$ cells that were generated in *Runx3*-transgenic thymi, we examined the marker expression in the HSA^{low} cells by RT-PCR analysis (Fig. 5*C*). A transcript of *perforin1*, a $CD4^-8^+$ marker (21), was clearly detected in the wild-type as well as *Runx3*-transgenic $CD4^-8^+$ cells, but detected only in a subtle amount in the $CD4^+8^-$ cells of both genotypes. In contrast, a transcript of *GATA3*, a $CD4^+8^-$ marker (21), was expressed more abundantly in the $CD4^+8^-$ cells than in the $CD4^-8^+$ cells irrespective of genotypes of cells. The results in Fig. 5 indicate that the overexpressed Runx3 in fact promoted the differentiation and maturation of thymocytes toward the CD8 lineage.

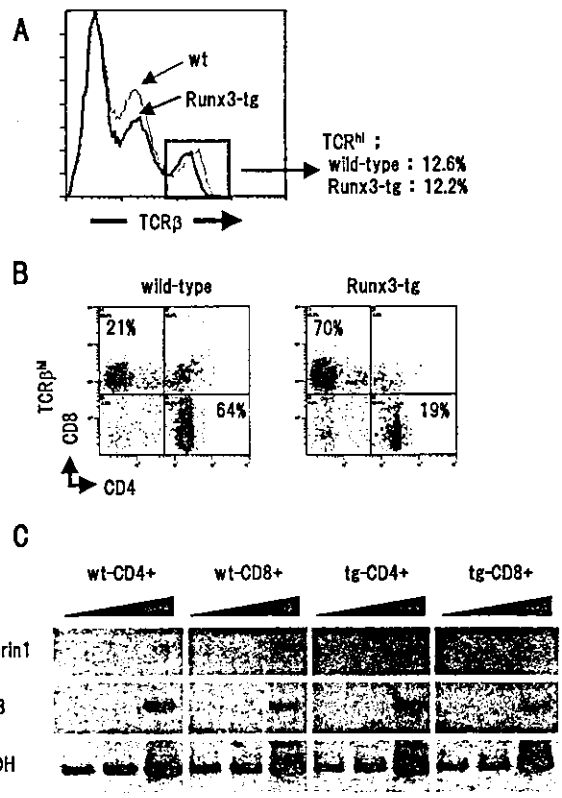

FIGURE 5. Effect of the *Runx3* transgene on the differentiation of mature, TCR^{high} cells. *A*, The thymocytes from wild-type and *Runx3*-transgenic mice were stained for TCR, and their expression profiles were analyzed. The cells were classified into three subpopulations: TCR^{low}, TCR^{med}, and TCR^{high}. *B*, The wild-type and *Runx3*-transgenic thymocytes were processed for three-color flow cytometrical analysis. The mature, TCR^{high} subpopulation was selected, and its CD8 and CD4 expression profile was analyzed. The numbers in the individual quadrants indicate the percentage of cells of each type. *C*, Semiquantitative RT-PCR analysis of *perforin1*, *GATA3*, and *G3PDH* transcripts. RNA was isolated from the $CD4^+8^-HSA^{low}$ and $CD4^-8^+HSA^{low}$ thymocytes' fractions and converted to cDNA. An increasing amount of cDNA synthesized from the wild-type and *Runx3*-transgenic cells, respectively, was processed for PCR.

The mature $CD4^-8^+$ cells are released into periphery of Runx3-transgenic mice

Promotion of thymocyte differentiation toward the CD8 lineage by Runx3 was also reflected in the cell composition in the spleen (Fig. 6, *A* and *B*). Among the $TCR^{high}HSA^{low}$ mature T cells, the ratio of $CD4^-8^+$ cells to $CD4^+8^-$ cells was 0.5 in the spleens from the wild type, but was 1.4 in the transgenic splenocytes.

We wondered whether the increase in mature $CD8^+$ cells reflected the preferential expansion of a specific repertoire of TCR. We therefore examined the usage of Vβ regions by the $TCR^{high}CD8^+$ splenocytes using flow cytometry (Fig. 6*C*). The pattern of the Vβ repertoire was essentially similar between the transgenic and wild-type cells. Therefore, in the *Runx3*-transgenic mice, apparently normal, multiclonal, mature $CD8^+$ cells were generated in the thymus and released into periphery as in the wild-type mice.

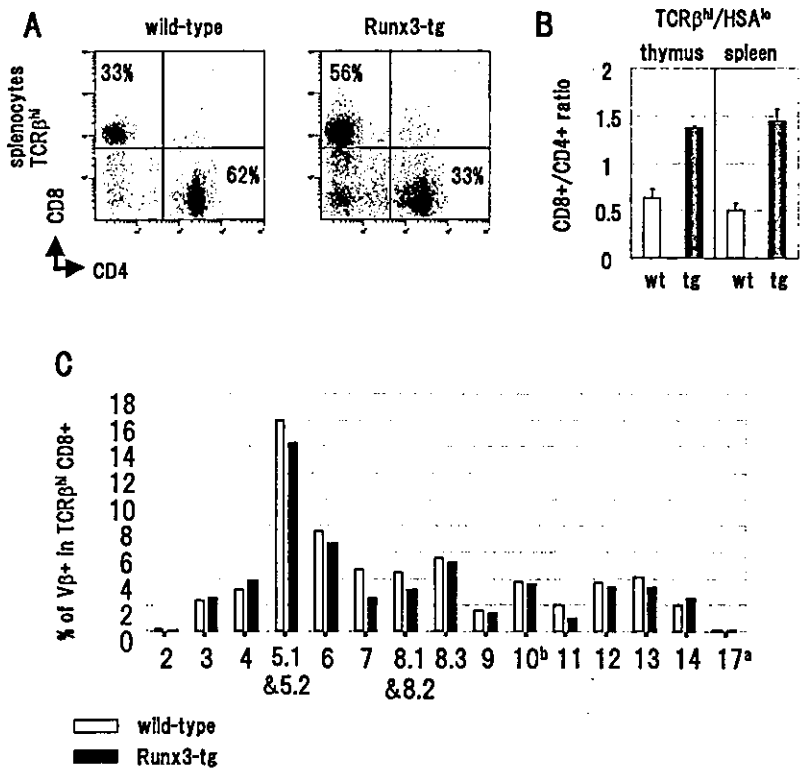

FIGURE 6. Effect of the *Runx3*-transgene on splenic T lymphocytes. *A*, The wild-type and *Runx3*-transgenic splenocytes were processed for three-color flow cytometrical analysis. The mature TCR^{high} subpopulation was selected, and its CD8 and CD4 expression profile was analyzed. The numbers in the individual quadrants indicate the percentage of cells of each type. *B*, The cell number ratios of $TCR^{high}HSA^{low}CD4^{-}8^{+}$ cells to $TCR^{high}HSA^{low}CD4^{+}8^{-}$ cells in the wild-type and *Runx3*-transgenic thymus and spleen. *C*, The Vβ repertoire used by the TCRs of splenic $CD4^{-}8^{+}$ cells. Wild-type (□) and *Runx3*-transgenic (■) cells were stained by an Ab mixture against various Vβ segments and processed for flow cytometrical analysis.

Overexpression of Runx3 can drive originally CD4-oriented thymocytes toward the CD8 lineage

The results shown in Figs. 5 and 6 indicate that the overexpressed Runx3 can drive thymocytes to select and mature along the CD8 lineage. We then examined whether this effect of Runx3 is dependent on the TCR signaling elicited from proper MHC interactions. The *TCR* transgene, which is restricted to MHC class II, was introduced into *Runx3* transgenic mice (Fig. 7*A*). Thymi from *TCR* single-transgenic mice showed a skew of cell differentiation to the CD4 lineage (33% $CD4^{+}8^{-}$ compared with 3.6% $CD4^{-}8^{+}$). In contrast, in the *TCR* and *Runx3* double-transgenic thymi, the $CD4^{-}8^{+}$ cells constituted the major population (73%), just as in the case of *Runx3*-single-transgenic thymi. When only the mature cells were selected by gating the HSA^{low} fraction (and by gating the transgene-specific TCR^{high} fraction as well (data not shown)), it was clear that the *Runx3* transgene switched the differentiation of class II-restricted cells to the CD8 lineage.

We further confirmed the cell-autonomous activity of Runx3 by altering the MHC background. The $\beta_2 m$ (−/−), class I-deficient thymus provides an environment unfavorable for the selection of $CD4^{-}8^{+}$ cells (Fig. 7*B*). In the TCR^{high} fraction, 90% of wild-type thymocytes were $CD4^{+}8^{-}$ cells. In contrast, the *Runx3* transgene appeared to shift the differentiation of thymocytes toward the CD8 lineage even in the context of class I deficiency. Thus, overexpressed Runx3 can push a cell toward the CD8 lineage independently of the MHC-elicited TCR signaling.

Overexpression of Runx3 can drive thymocytes toward the CD8 lineage irrespective of the CD4 signaling

In thymocyte differentiation, the TCR signaling exerts its effect in concert with the signaling elicited from either the CD4 or CD8 molecule. We examined the activity of overexpressed Runx3 on thymocyte differentiation under the condition of either excess or deficiency of CD4 signaling. First, the *Runx3*-transgene was introduced into human *CD4*-transgenic mice (Fig. 8*A*). As seen, the level of human CD4 expression was not so high and therefore might be limited to compensate the endogenous, murine CD4, which should be silenced by the overexpressed Runx3. Under this limitation, a majority of mature TCR^{high} cells possessed a $CD4^{-}8^{+}$ phenotype in *Runx3*-transgenic thymi. Second, the *Runx3*-transgene was expressed in a *CD4*-deficient background (Fig. 8*B*). When a $CD4^{-}8^{+}$ fraction was displayed for its TCR expression, the mature TCR^{high} cells corresponded to 27% of *CD4*-deficient and *Runx3*-transgenic thymocytes. In contrast, such mature cells occupied only 17% of simple *CD4*-deficient thymocytes. Collectively, neither an excess nor a lack of CD4 signaling appears to influence the extent of overproduction of mature $CD4^{-}8^{+}$ thymocytes, which is caused by the overexpressed Runx3. Thus, the activity of Runx3 to drive thymocytes toward the CD8 lineage is likely to be due to more than a simple silencing of *CD4* gene expression.

Discussion

Whether DP thymocytes select the CD8 or CD4 lineage is determined by the strength and/or duration of the TCR signal the cells receive through their interactions with an MHC/peptide complex (7, 22, 23). The DP cells cease expressing either the *CD4* or *CD8* gene, and thus eventually become committed to the CD8 SP or CD4 SP lineage, respectively. A *CD4* silencer element and the Runx binding sites in it play a pivotal role in the cessation of *CD4* expression (13, 24). Based on the analysis of thymocytes lacking *Runx1* or *Runx3*, Taniuchi et al. (13) proposed that Runx1 functions as an active repressor of *CD4* expression at the DN stage, whereas Runx3 is involved in the epigenetic silencing of the gene at the CD8 SP stage.

In the present study, we created *Runx3*-transgenic mice and found that the number of mature $CD4^{-}8^{+}$ thymocytes was increased. This result is opposite to that found in the *Runx3* (−/−) thymus, in which the number of mature $CD4^{-}8^{+}$ cells is markedly

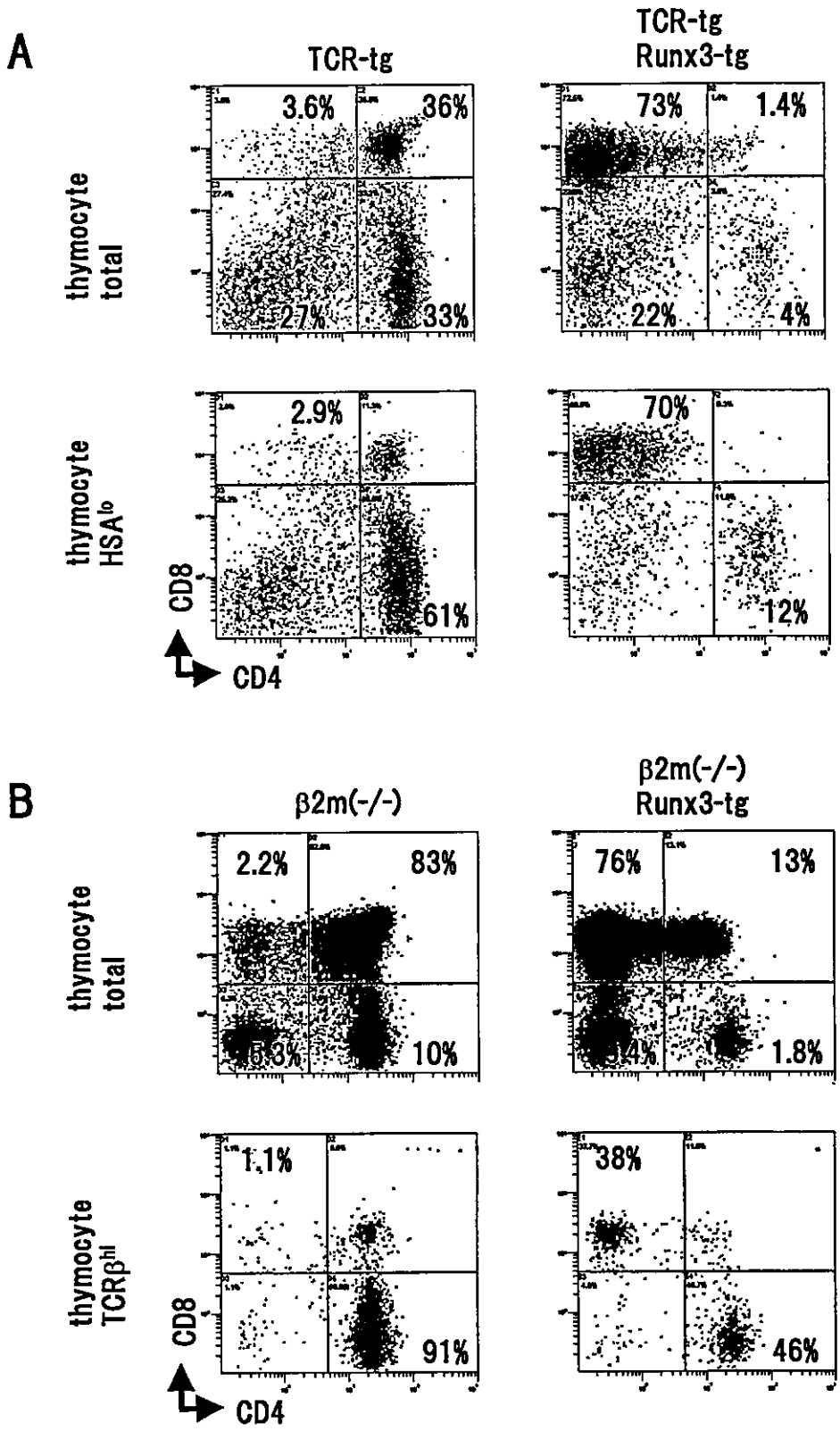

FIGURE 7. Effect of Runx3 overexpression on the differentiation potential of CD4-oriented thymocytes. *A*, The *TCR* transgene restricted to class II (*left*) was introduced into *Runx3*-transgenic mice (*right*). The CD4/CD8 expression profiles are shown for the nongated thymocytes (*upper panels*) as well as the mature, HSA^{low} thymocytes (*lower panels*). *B*, MHC class I deficiency (*left*) and the same deficiency coupled with the *Runx3*-transgene (*right*). The CD4/CD8 expression profiles are shown for the nongated thymocytes (*upper panels*) as well as the mature, TCR^{high} thymocytes (*lower panels*). The numbers in individual quadrants represent the percentages of cells of each type.

decreased (13, 14). Therefore, the present gain-of-function analysis complements the previous loss-of-function analysis. However, a close inspection of our results reveals a new aspect of Runx3 function as described below and as summarized in Fig. 9.

In the *Runx3*-transgenic thymus, the absolute number of mature $CD4^-8^+$ thymocytes was increased 2-fold compared with the nontransgenic thymus. This phenomenon cannot be explained solely by the effect of Runx3 on the *CD4* silencer. If *CD4* silencing had been overwhelming in the *Runx3*-transgenic mice, then the mature $CD4^+8^-$ thymocytes might also lose *CD4* expression, and a significant number of $CD4^-8^-TCR^{high}$ thymocytes might have been generated. However, we did not see evidence of such a population in the transgenic thymus. Mice lacking the *CD4* gene itself lose *CD4* expression completely, and the number of mature $CD4^-8^+$

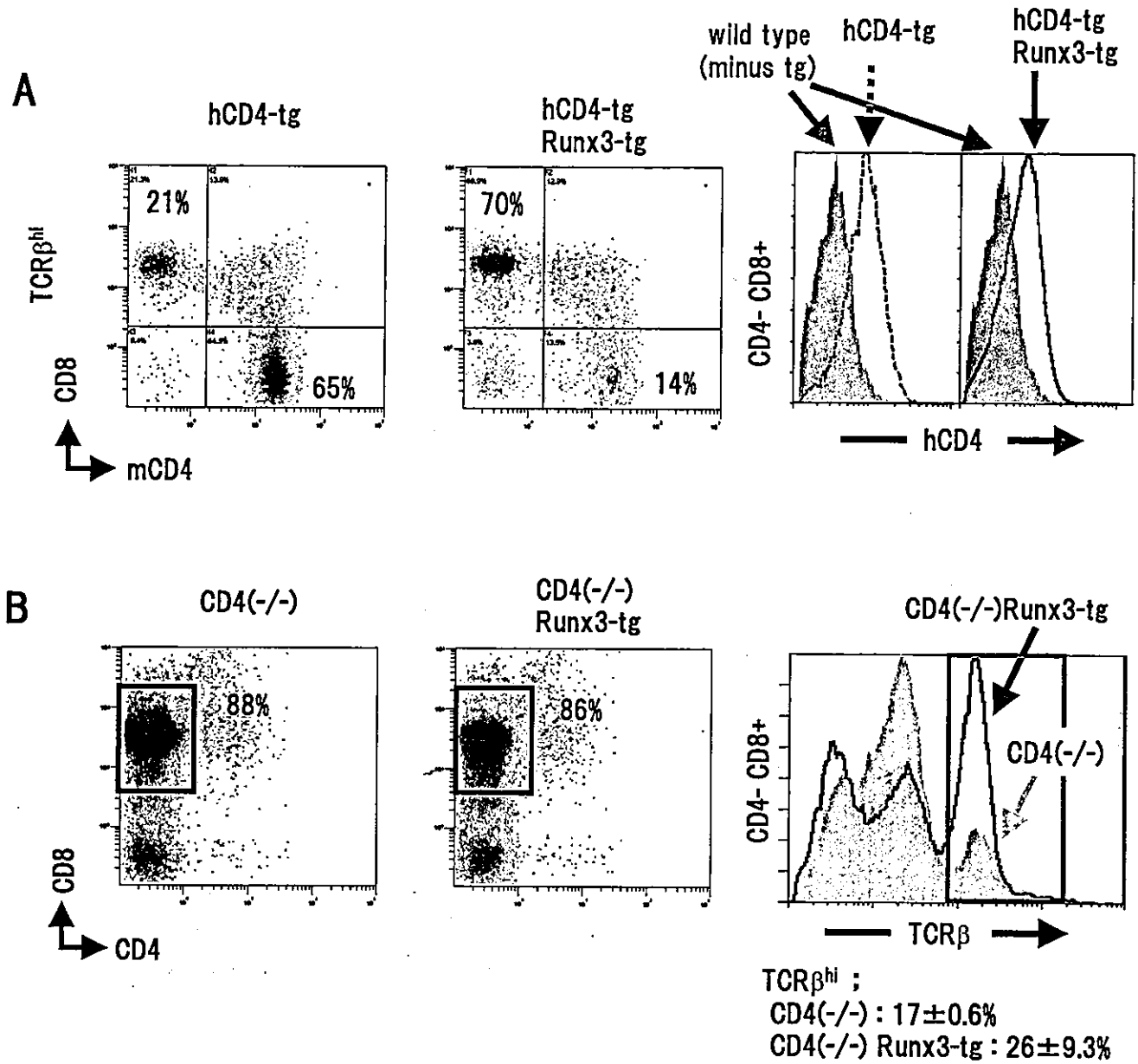

FIGURE 8. Effects of human *CD4* transgene and/or endogenous murine *CD4* deficiency on the differentiation of *Runx3*-transgenic thymocytes. *A*, The human *CD4* transgene driven by the murine *CD4* enhancer/promoter (*left*) was introduced into *Runx3*-transgenic mice (*middle*). The murine CD4/CD8 expression profiles are shown for the mature, TCR^{high} thymocytes (*left* and *middle*). In the *right panel*, the expression profiles of human CD4 are displayed for the murine $CD4^-8^+$ thymocytes. The shaded peak represents the wild-type cells, whereas the open peak represents the human *CD4*-single- and the human *CD4*- and *Runx3*-double-transgenic cells, respectively. *B*, A murine *CD4* deficiency (*left*) and the same deficiency coupled with the *Runx3*-transgene (*middle*). The CD4/CD8 expression profiles are shown for the nongated thymocytes (*left* and *middle*). In the *right panel*, the expression profiles of TCR are displayed for the gated $CD4^-8^+$ fraction. The shaded peak represents *CD4* (−/−) mice, whereas the open peak represents *CD4* (−/−):*Runx3*-transgenic mice.

thymocytes does not vary from that of wild-type mice (25). In contrast, we observed that overexpression of Runx3 could more efficiently convert the *CD4* (−/−) thymocytes to the mature $CD8^+$ cells. A similar result was obtained for the *Runx3*- and class II-restricted *TCR* double-transgenic mice as well as *Runx3*-transgenic:β_2m (−/−) mice. Taken together, Runx3 likely possesses the capacity not only to suppress *CD4* gene expression but also to actively drive the thymocytes toward the CD8 lineage.

In the wild-type thymus, the endogenous Runx3 is likely involved in the selection of and commitment to the CD8 lineage in concert with TCR signaling. A short and/or weak TCR signal is somehow transduced to Runx3, which in turn regulates the gene expression necessary for the CD8 lineage determination. *CD4* silencing is one target of Runx3 (13) and maintenance of *CD8* expression is probably a target as well. Another possibility is that Runx3 is involved in the survival and/or maturation of thymocytes after they have selected the CD8 lineage.

At the DN stage, the *CD4* silencer is reported to be "ON." Transcription of the *CD4* gene is initiated when the DN cells move to the DP stage, and the activity of the *CD4* silencer is expected to be turned "OFF" during the transition from DN to DP (26). The mechanism of this "OFF" switch cannot be assessed by targeted deletions of *Runx3* or *CD4* silencer. In our *Runx3*-transgenic thymus, the percentage and number of $CD4^+8^+$ cells were

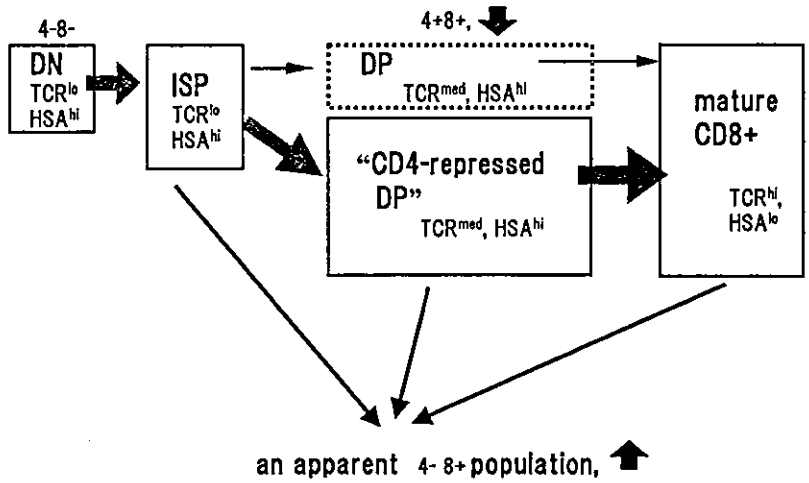

FIGURE 9. A model of T lymphocyte differentiation in the *Runx3*-transgenic thymus. Each step of differentiation is characterized by the specific expression patterns of CD4, CD8, TCR, and HSA. The cells usually start at the DN stage, go through the ISP and DP stages, and mature at the CD8 SP stage. The "CD4-repressed DP" stage is characterized by TCR^{med} expression; is apparently categorized as a $CD4^-8^+$ fraction; and is observed only in the *Runx3*-transgenic, but not the wild-type, thymus. The majority of mature $TCR^{high}HSA^{low}CD4^-8^+$ cells are considered to be derived from the premature "CD4-repressed DP" cells. A minor pathway for $CD8^+$ maturation in the transgenic animals would be through the usual "DP" stage.

remarkably reduced, and an aberrant population of "CD4-repressed DP" cells with a $CD4^-8^+TCR^{med}HSA^{high}$ phenotype emerged instead. It is likely that exogenous expression of the transgene-derived Runx3 protein maintained the *CD4* silencer in the "ON" position, thereby giving rise to the "CD4-repressed DP" thymocytes from the immature $CD4^-8^+TCR^{low}$ cells. However, these premature cells do acquire a $CD4^-8^+$ phenotype, probably due to the strong repression of *CD4* expression.

We previously reported the phenotype of *Runx1*-transgenic mice in which the numbers of both immature ISP and mature CD8 SP cells were increased (9). Even taking into consideration the differences between the *Runx3*- and *Runx1*-transgenic thymocytes in terms of the promoters used and/or the magnitude of transduced protein expression, it is interesting to note that overexpression of Runx1 did not generate the "CD4-repressed DP" cells as Runx3 did. Furthermore, the endogenous Runx1 protein is easily detected in the DP cells of wild-type thymus (10, 11), and Runx1 and Runx3 do not associate with each other in a coimmunoprecipitation experiment (K. Kohu and M. Satake, unpublished data). These observations suggest both that Runx1 is not involved in the turning the *CD4* silencer "OFF" at the DP stage and that the overexpressed Runx3 can reactivate the *CD4* silencer at this DP stage. It must be noted, though, that the enforced expression of Runx1 in a fetal thymic organ culture could generate similar "CD4-repressed DP" cells (27). The mechanism by which the *CD4* silencer is turned "OFF" at the DN-to-DP transition needs further investigation.

The *Runx3*-transgenic thymus clearly contained mature $CD4^+8^-$ cells, and we confirmed that the transduced Runx3 was indeed expressed in these cells. Perhaps in thymocytes that are committed to the $CD4^+8^-$ lineage, the chromatin structure at the *CD4* silencer region may be in a "closed" state, denying Runx3 access to the site.

Several transcription factors have been reported to be involved in the lineage selection of CD4/8 thymocytes. GATA3 is a positive regulator that boosts thymocytes toward the CD4 lineage (28–30), whereas TOX (31, 32) and/or activated Notch1 (33) move thymocytes toward the CD8 lineage. These factors are thought to function in response to an adequate signal from TCR when expressed endogenously, but transgenic overexpression might reveal cell-autonomous aspects of their functions. Thus, the possible interplay between the TCR signal, TOX, and Runx3 in the CD8 lineage selection will be a fascinating subject to pursue.

Acknowledgments

We are grateful to the following scientists for providing us with the valuable experimental tools: Y. Groner and D. Levanon for the murine *Runx3* cDNA, and R. Perlmutter for the proximal *Lck*-promoter. We express our thanks to M. Kuji for her secretarial assistance.

Disclosures

The authors have no financial conflict of interest.

References

1. Anderson, G., B. C. Harman, K. J. Hare, and E. J. Jenkinson. 2000. Microenvironmental regulation of T cell development in the thymus. *Semin. Immunol. 12:457.*
2. Varas, A., A. L. Hager-Theodorides, R. Sacedon, A. Vicente, A. G. Zapata, and T. Crompton. 2003. The role of morphogens in T-cell development. *Trends Immunol. 24:197.*
3. Basson, M. A., and R. Zamoyska. 2000. The CD4/CD8 lineage decision: integration of signalling pathways. *Immunol. Today 21:509.*
4. Germain, R. N. 2002. T-cell development and the CD4-CD8 lineage decision. *Nat. Rev. Immunol. 2:309.*
5. Alberola-Ila, J., and G. Hernandez-Hoyos. 2003. The Ras/MAPK cascade and the control of positive selection. *Immunol. Rev. 191:79.*
6. Rothenberg, E. V. 2002. T-lineage specification and commitment: a gene regulation perspective. *Semin. Immunol. 14:431.*
7. Singer, A. 2002. New perspectives on a developmental dilemma: the kinetic signaling model and the importance of signal duration for the CD4/CD8 lineage decision. *Curr. Opin. Immunol. 14:207.*
8. Hayashi, K., W. Natsume, T. Watanabe, N. Abe, N. Iwai, H. Okada, Y. Ito, M. Asano, Y. Iwakura, S. Habu, et al. 2000. Diminution of the AML1 transcription factor function causes differential effects on the fates of CD4 and CD8 single-positive T cells. *J. Immunol. 165:6816.*
9. Hayashi, K., N. Abe, T. Watanabe, M. Obinata, M. Ito, T. Sato, S. Habu, and M. Satake. 2001. Overexpression of AML1 transcription factor drives thymocytes into the CD8 single-positive lineage. *J. Immunol. 167:4957.*
10. Ehlers, M., K. Laule-Kilian, M. Petter, C. J. Aldrian, B. Grueter, A. Wurch, N. Yoshida, T. Watanabe, M. Satake, and V. Steimle. 2003. Morpholino antisense oligonucleotide-mediated gene knockdown during thymocyte development reveals role for Runx3 transcription factor in CD4 silencing during development of $CD4^-/CD8^+$ thymocytes. *J. Immunol. 171:3594.*
11. Sato, T., R. Ito, S. Nunomura, S. Ohno, K. Hayashi, M. Satake, and S. Habu. 2003. Requirement of transcription factor AML1 in proliferation of developing thymocytes. *Immunol. Lett. 89:39.*
12. Ichikawa, M., T. Asai, T. Saito, G. Yamamoto, S. Seo, I. Yamazaki, T. Yamagata, K. Mitani, S. Chiba, H. Hirai, et al. 2004. AML-1 is required for megakaryocytic maturation and lymphocytic differentiation, but not for maintenance of hematopoietic stem cells in adult hematopoiesis. *Nat. Med. 10:229.*
13. Taniuchi, I., M. Osato, T. Egawa, M. J. Sunshine, S. C. Bae, T. Komori, Y. Ito, and D. R. Littman. 2002. Differential requirements for Runx proteins in CD4 repression and epigenetic silencing during T lymphocyte development. *Cell 111:621.*
14. Woolf, E., C. Xiao, O. Fainaru, J. Lotem, D. Rosen, V. Negreanu, Y. Bernstein, D. Goldenberg, O. Brenner, G. Berke, et al. 2003. Runx3 and Runx1 are required for CD8 T cell development during thymopoiesis. *Proc. Natl. Acad. Sci. USA 100:7731.*
15. Levanon, D., V. Negreanu, Y. Bernstein, I. Bar-Am, L. Avivi, and Y. Groner. 1994. AML1, AML2, and AML3, the human members of the runt domain gene-family: cDNA structure, expression, and chromosomal localization. *Genomics 23:425.*
16. Garvin, A. M., K. M. Abraham, K. A. Forbush, A. G. Farr, B. L. Davison, and R. M. Perlmutter. 1990. Disruption of thymocyte development and lymphomagenesis induced by SV40 T-antigen. *Int. Immunol. 2:173.*
17. Sato, T., T. Sasahara, Y. Nakamura, T. Osaki, T. Hasegawa, T. Tadakuma, Y. Arata, Y. Kumagai, M. Katsuki, and S. Habu. 1994. Naive T cells can mediate

delayed-type hypersensitivity response in T cell receptor transgenic mice. *Eur. J. Immunol. 24:1512.*
18. Chiba, N., T. Watanabe, S. Nomura, Y. Tanaka, M. Minowa, M. Niki, R. Kanamaru, and M. Satake. 1997. Differentiation dependent expression and distinct subcellular localization of the protooncogene product, PEBP2β/CBFβ, in muscle development. *Oncogene 14:2543.*
19. Kanto, S., N. Chiba, Y. Tanaka, S. Fujita, M. Endo, N. Kamada, K. Yoshikawa, A. Fukuzaki, S. Orikasa, T. Watanabe, and M. Satake. 2000. The PEBP2β/CBFβ-SMMHC chimeric protein is localized both in the cell membrane and nuclear subfractions of leukemic cells carrying chromosomal inversion 16. *Leukemia 14:1253.*
20. Tanaka, Y., T. Watanabe, N. Chiba, M. Niki, Y. Kuroiwa, T. Nishihira, S. Satomi, Y. Ito, and M. Satake. 1997. The protooncogene product, PEBP2β/CBFβ, is mainly located in the cytoplasm and has an affinity with cytoskeletal structures. *Oncogene 15:677.*
21. Liu, X., and R. Bosselut. 2004. Duration of TCR signaling controls CD4-CD8 lineage differentiation in vivo. *Nat. Immunol. 5:280.*
22. Yasutomo, K., C. Doyle, L. Miele, C. Fuchs, and R. N. Germain. 2000. The duration of antigen receptor signalling determines $CD4^+$ versus $CD8^+$ T-cell lineage fate. *Nature 404:506.*
23. Hogquist, K. A. 2001. Signal strength in thymic selection and lineage commitment. *Curr. Opin. Immunol. 13:225.*
24. Zou, Y. R., M. J. Sunshine, I. Taniuchi, F. Hatam, N. Killeen, and D. R. Littman. 2001. Epigenetic silencing of CD4 in T cells committed to the cytotoxic lineage. *Nat. Genet. 29:332.*
25. Rahemtulla, A., W. P. Fung-Leung, M. W. Schilham, T. M. Kundig, S. R. Sambhara, A. Narendran, A. Arabian, A. Wakeham, C. J. Paige, R. M. Zinkernagel, et al. 1991. Normal development and function of $CD8^+$ cells but markedly decreased helper cell activity in mice lacking CD4. *Nature 353:180.*
26. Sawada, S., J. D. Scarborough, N. Killeen, and D. R. Littman. 1994. A lineage-specific transcriptional silencer regulates *CD4* gene expression during T lymphocyte development. *Cell 77:917.*
27. Telfer, J. C., E. E. Hedblom, M. K. Anderson, M. N. Laurent, and E. V. Rothenberg. 2004. Localization of the domains in Runx transcription factors required for the repression of CD4 in thymocytes. *J. Immunol. 172:4359.*
28. Nawijn, M. C., R. Ferreira, G. M. Dingjan, O. Kahre, D. Drabek, A. Karis, F. Grosveld, and R. W. Hendriks. 2001. Enforced expression of GATA-3 during T cell development inhibits maturation of CD8 single-positive cells and induces thymic lymphoma in transgenic mice. *J. Immunol. 167:715.*
29. Hernandez-Hoyos, G., M. K. Anderson, C. Wang, E. V. Rothenberg, and J. Alberola-Ila. 2003. GATA-3 expression is controlled by TCR signals and regulates CD4/CD8 differentiation. *Immunity 19:83.*
30. Pai, S. Y., M. L. Truitt, C. N. Ting, J. M. Leiden, L. H. Glimcher, and I. C. Ho. 2003. Critical roles for transcription factor GATA-3 in thymocyte development. *Immunity 19:863.*
31. Wilkinson, B., J. Y. Chen, P. Han, K. M. Rufner, O. D. Goularte, and J. Kaye. 2002. TOX: an HMG box protein implicated in the regulation of thymocyte selection. *Nat. Immunol. 3:272.*
32. Aliahmad, P., E. O'Flaherty, P. Han, O. D. Goularte, B. Wilkinson, M. Satake, J. D. Molkentin, and J. Kaye. 2004. TOX provides a link between calcineurin activation and CD8 lineage commitment. *J. Exp. Med. 199:1089.*
33. Robey, E., D. Chang, A. Itano, D. Cado, H. Alexander, D. Lans, G. Weinmaster, and P. Salmon. 1996. An activated form of Notch influences the choice between CD4 and CD8 T cell lineages. *Cell 87:483.*

DNA RESEARCH 11, 335–344 (2004)

Gene Expression Profiling Identifies a Set of Transcripts that are Up-Regulated in Human Testicular Seminoma

Shigeyuki YAMADA,[1,2] Kazuyoshi KOHU,[1] Tomohiko ISHII,[1,2] Shigeru ISHIDOYA,[2] Masayoshi HIRAMATSU,[2] Satoru KANTO,[2] Atsushi FUKUZAKI,[2] Yutsu ADACHI,[3] Mareyuki ENDOH,[3] Takuya MORIYA,[3] Hiroki SASAKI,[4] Masanobu SATAKE,[1,*] and Yoichi ARAI[2]

Department of Molecular Immunology, Institute of Development, Aging and Cancer, Tohoku University, Seiryo-machi 4-1, Aoba-ku, Sendai 980-8575, Japan,[1] Department of Urology, Graduate School of Medicine, Tohoku University, Seiryo-machi 1-1, Aoba-ku, Sendai 980-8574, Japan,[2] Department of Pathology, Graduate School of Medicine, Tohoku University, Seiryo-machi 1-1, Aoba-ku, Sendai 980-8574, Japan,[3] and Genetics Division, National Cancer Center Research Institute, Tsukiji 5-1-1, Chuo-ku, Tokyo 104-0045, Japan[4]

(Received 17 July 2004; revised 20 August 2004)

Abstract

Seminoma constitutes one subtype of human testicular germ cell tumors and is uniformly composed of cells that are morphologically similar to the primordial germ cells and/or the cells in the carcinoma *in situ*. We performed a genome-wide exploration of the genes that are specifically up-regulated in seminoma by oligonucleotide-based microarray analysis. This revealed 106 genes that are significantly and consistently up-regulated in the seminomas compared to the adjacent normal tissues of the testes. The microarray data were validated by semi-quantitative RT-PCR analysis. Of the 106 genes, 42 mapped to a small number of specific chromosomal regions, namely, 1q21, 2p23, 6p21-22, 7p14-15, 12p11, 12p13, 12q13-14 and 22q12-13. This list of up-regulated genes may be useful in identifying the causative oncogene(s) and/or the origin of seminoma. Furthermore, immunohistochemical analysis revealed that the seminoma cells specifically expressed the six gene products that were selected randomly from the list. These proteins include CCND2 and DNMT3A and may be useful as molecular pathological markers of seminoma.

Key words: testicular seminoma; gene expression; microarray analysis; immunohistochemistry

1. Introduction

Human testicular tumors of germ cell origin are histologically classified into two major groups, namely, seminomas and non-seminomas. These two types of tumors have an invasive phenotype and are believed to be derived from a common ancestor, carcinoma *in situ* (CIS), where the generation and expansion of tumor cells is limited to within the seminiferous tubules. Non-seminomas, such as embryonal carcinoma and teratoma, contain stem cells as well as cells that have differentiated toward somatic lineages to various degrees, thus giving rise to a morphologically pleiotropic appearance. In contrast, seminomas have a rather uniform appearance, at least at the histological level. Due to this apparently homogenous cell composition, seminomas are particularly suitable for investigations of tumor-associated alterations in gene expression. In addition, the cells that constitute seminomas resemble the primordial germ cells and/or the cells in the CIS. Thus, gene expression profiling of seminomas is interesting not only with regard to understanding their oncogenesis, it may also be useful for research into primordial germ cells.

Many reports have described cytogenetic and molecular abnormalities associated with testicular germ cell tumors.[1,2] These abnormalities include: aneuploidy (near triploidy is most common);[3–5] the gain and/or loss of some specific chromosomal regions such as the presence of iso-chromosome 12p;[6–8] the amplification of 12p sequences;[9,10] the gain of chromosomal material in 1, 2p, 7, 8, 12, 14q, 15q, 17q, 21q and X or the deletion of chromosomal material from 4, 5, 11q, 13q and 18q;[2] the alteration of expression of genes located on chromosomes 12p and 17q;[11–13] and the up-regulation of several specific genes, including *cyclin D2* (*CCND2*).[14–18] Despite these observations, the exact molecular mechanism(s) behind the carcinogenesis of germ cells and their progression is still poorly understood. In the present study, we per-

Communicated by Misao Ohki

* To whom correspondence should be addressed. Tel. +81-22-717-8477, Fax. +81-22-717-8482, E-mail: satake@idac.tohoku.ac.jp

formed a genome-wide profiling of the gene expression in seminomas by oligonucleotide-based microarray analysis. We identified 106 genes that are specifically up-regulated in seminomas. These represent candidate genes that may indicate the origin of seminomas and/or may be responsible for the development of seminomas. In addition, we showed by immunohistochemical analysis that seminoma cells but not normal testicular cells stain positively for the products of several of these genes. Thus, these proteins may be useful as molecular pathological markers of the tumors.

2. Materials and Methods

2.1. RNA isolation

Testicular tissues surgically dissected from patients were kept frozen at −80°C until use. The use of these samples for gene analysis was approved by the Committee for Medical Research of the Graduate School of Medicine, Tohoku University (2002-082). The tissues were homogenized in Trizol (Life Technologies Inc., Rockville, MD) and extracted with chloroform, and the RNA was precipitated by isopropanol. The RNA pellet was then dissolved in RNase-free water. The quality of the RNA was analyzed by an RNA LabChip (Caliper Technologies Corp., CA).

2.2. Microarray Analysis

cDNA was synthesized from 5 μg of RNA by reverse transcriptase and then biotinylated cRNA was synthesized from the cDNA using T7-RNA polymerase. The fragmented cRNA (10 μg) was then hybridized to human genome U133A oligonucleotide probe arrays (Affymetrix, Santa Clara, CA) that cover roughly 20,000 independent genes. The hybridization was performed at 45°C for 16 hr in a specific cocktail. Washing and staining was done according to the protocol supplied by the manufacturer. The arrays were scanned by an HP Gene Array Scanner (Affymetrix) at a resolution of 3 μm. The images thus obtained were analyzed quantitatively with Microarray Suite 4.0 software (Affymetrix) to yield the raw signal intensity data. When detection calls were marginal or absent, their signal intensities were taken as 1. In order to compare mRNA expression levels among samples, we normalized the raw data by setting the mean of the signal intensities of all probe sets in each sample to 1,000. The signal intensities thus normalized were average difference scores and used in the following analysis. To statistically analyze the gene signal intensities, Microsoft Excel was used, while Cluster and Tree View at http://rana.lbl.gov/EisenSoftware.htm were used for cluster analysis.

2.3. RT-PCR analysis

Semi-quantitative RT-PCR analysis was performed with 1 μg cDNA. Forward and reverse primers were designed for each of the transcripts examined using the Genetyx Mac 9.0/search primer software. The sequences of the forward and reverse primers used are presented in supplementary Table 1, http://www.dna-res.kazusa.or.jp/11/5/03/supplement_table/table1.html. The polymerase that was used was ExTaq (Takara, Otsu, Japan) and PCR was performed for each transcript with 25, 27 or 30 cycles using the appropriate annealing temperature. PCR products were run through an agarose gel and their relative intensity compared to the internal DNA marker was determined using the NIH Image 1.63 software (http://rsb.info.nih.gov/nih-image/download.html).

2.4. Immunohistochemistry

Testis specimens were fixed in 4% (wt/vol) paraformaldehyde in PBS for 18 hr at 4°C and embedded in paraffin. Micro-sectioned specimens on slides were then de-paraffinized and processed for immunohistochemical staining. The primary antibodies used were anti-DNMT3A (sc-10231), anti-SOX4 (sc-17326), anti-CCND2 (sc-181G), anti-ACVR1B (42222), anti-FGD1 (sc-11109) and anti-PIM2 (sc-13675). Anti-ACVR1B was purchased from Techne whereas the other antibodies were from Santa Cruz Biotech. Inc., Santa Cruz, CA. The antibodies were used at an appropriate dilution and the immune-complexes were detected using a Histofine kit (Nichirei, Tokyo, Japan). The kit employs a streptoavidin/biotin amplification method. The specimens were counter-stained with methyl green.

3. Results

3.1. Selection of seminoma samples and adjacent normal tissues

Eight testes were surgically dissected from patients suffering from seminoma (Table 1). The samples were numbered patient (Pt.) 1 through to Pt. 8. In addition, one apparently normal testis was obtained from Pt. 9, who suffered from prostate cancer and received bilateral orchiectomy.

In the case of Pts. 5–8, the entire testes were invaded by the tumor cells. In contrast, in the case of Pts. 1–4, tumor and adjacent normal regions could be macroscopically distinguished from each other and were separated from each other. Thus, we isolated 13 different kinds of RNAs from testes, namely, RNAs prepared from the adjacent normal tissues and the tumor portions of Pts. 1–4, RNAs prepared from the tumors of Pts. 5–8 and RNA from the normal testis of Pt. 9. All of the RNAs were processed for microarray analysis.

Table 1. Clinical data of patients and RNA preparation from seminoma.[a]

Patient number[b]	Patient age	Clinical stage[c]	Carcinoma *in situ*[d]	AFP[e] (ng/ml)	HCG[f] (mIU/ml)	HCG-β (ng/ml)	LDH (IU/L)	RNA preparation[g]
Pt. 1	27	Is	not detected	2.3	3	0.04	n.e.	Pt. 1-T, Pt. 1-N
Pt. 2	44	Is	not detected	4.3	16	0.3	336	Pt. 2-T, Pt. 2-N
Pt. 3	41	Is	detected	1.6	1	0.9	5,035	Pt. 3-T, Pt. 3-N
Pt. 4	28	IIIb	detected	n.e.	n.e.	n.e.	1,267	Pt. 4-T, Pt. 4-N
Pt. 5	35	IIIb		4	202	5.4	1,124	Pt. 5-T
Pt. 6	42	IIIb		5.9	n.e.	1.6	938	Pt. 6-T
Pt. 7	45	Is		5.9	52	0.6	446	Pt. 7-T
Pt. 8	33	IIIb		2.1	295	1.1	8,324	Pt. 8-T
Pt. 9	65	normal[h]						Pt. 9-N

[a]Abbreviations used are Pt., patient; AFP, alpha-fetoprotein; HCG, human chorionic gonadotropin; HCG-β, human chorionic gonado-tropin beta; LDH, lactate dehydrogenase; n.e., not examined.
[b]At the time of surgery, patients did not receive any medication of anti-cancer drugs nor irradiation.
[c]The clinical stage of seminoma was based on the tumor, nodes and metastasis staging system employed by the American Joint Committee on Cancer staging.
[d]Presence or absence of carcinoma *in situ* in the adjacent normal regions of testes from the patient 1 through to 4 was examined histologically.
[e]AFP is an indication of yolk sac tumor and its serum level was low in most of the patients examined.
[f]A moderate level of HCG in sera of Pt. 5 and Pt. 8 is probably due to the presence of syncytiotrophoblastic giant cells that are scattered in the seminoma tissues.
[g]In the cases of patient 1 through to 4, RNA was prepared from the tumorous (T) and adjacent normal (N) regions of testes, whereas, in each case of patient 5 through to 8, the entire testis appeared to be occupied with the tumor cells (T).
[h]The patient 9 suffered from a prostate cancer and received bilateral orchiectomy. The testis showed no pathological alteration.

3.2. Screening for up-regulated genes in seminomas

For the paired RNA samples of Pts. 1–4, the signal intensity of the tumor region-derived RNA was divided by that of RNA from the adjacent normal tissue. These T/N ratios were thus calculated for four pairs of RNAs and for each probe. The probes that showed a T/N ratio that exceeded 3.0 for all four patients were selected for further analysis. Of the 20,000 probes, 115 met these criteria. Their details are shown in supplementary Table 2, http://www.dna-res.kazusa.or.jp/11/5/03/supplement_table/table2.html. In this table, the gene names are aligned according to their chromosomal map location. The numbers therein represent normalized signal intensities. It must be noted that the signal intensities obtained with the RNAs of Pts. 5–9 were not used during the course of gene extraction.

We then performed a cluster analysis of all 13 different kinds of RNA using the 115 probes we had extracted. A dendrogram depicting the neighboring relatedness of RNA samples is presented at the top of Fig. 1. This indicates that the RNAs from seminomas and those from the adjacent normal tissues are clearly divided into separate groups. This separation can also be recognized in a matrix format presentation of cluster analysis (see the separation of red and green dots into the tumor-derived and adjacent normal tissue-derived RNAs, respectively). Thus, the genes that were selected according to the criteria described above probably represent those with higher expression in seminomas than in normal testes.

Multiple probes were sometimes used for a single gene (supplementary Table 2, http://www.dna-res.kazusa.or.jp/11/5/03/supplement_table/table2.html). *TUBB*, *SOX4*, *OSBPL3*, *DDX11*, *CCND2*, *FKBP4* and *SLC23A1* are examples of this. Taking these overlaps into consideration reduced the 115 probes to 106 distinct genes. We next analyzed these 106 genes by plotting the number that are present on the short (p) and long (q) arms of each chromosome (Fig. 2A). This revealed that the 106 genes tended to cluster on several specific chromosomes such as 1q, 2p, 6p, 7p, 12p, 12q and 22q. Furthermore, we found by inspecting map location of the genes that 42 of the 106 up-regulated genes appear to be concentrated macroscopically on eight distinct chromosomal regions (see the 42 genes which are indicated by coloring in supplementary Table 2, http://www.dna-res.kazusa.or.jp/11/5/03/supplement_table/table2.html). Thus, four genes map on 1q21, three on 2p23, eight on 6p21-22, six on 7p14-15, four on 12p11, seven on 12p13, six on 12q13-14, and four on 22q12-13. We actually measured the distance between the neighboring genes and found that the average distance between the genes which were grouped as "concentrated" is 3,820 kilobases (±4,590, n=34), whereas the average distance between the genes which were grouped as "scattered" is 19,300 kilobases (±17,600, n=35). A difference between the two values is significant by a T-test ($p = 4.81 \times 10^{-6}$).

Of these 42 genes, we chose 19 genes for further analysis since their putative functions are relatively well an-

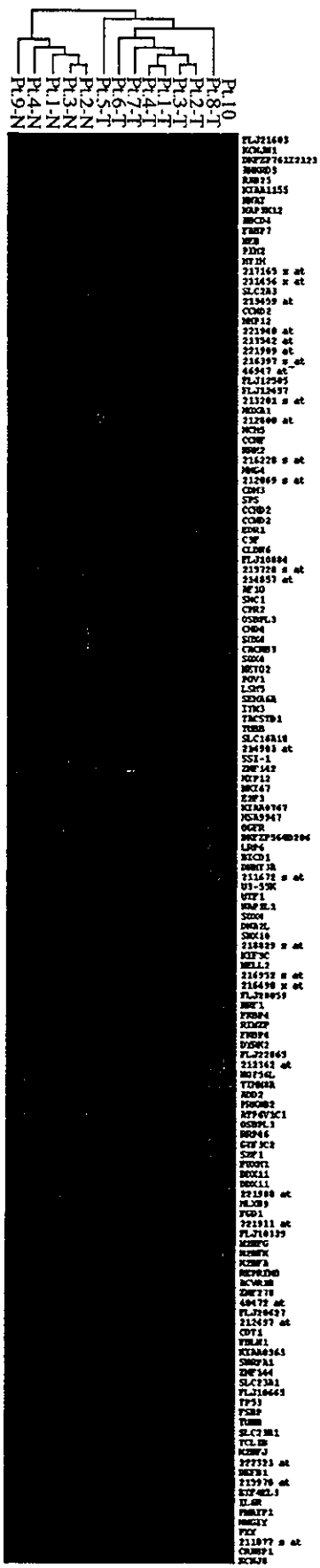

notated in the database and they are interesting from a biological perspective. We also analyzed the two genes that occur on Xp. Thus, 21 genes in total were analyzed further.

3.3. *Verification by RT-PCR of highly expressed genes in seminomas*

We sought to verify the microarray data by measuring the relative expression of the 21 genes by semi-quantitative RT-PCR. Thus, cDNA was synthesized from the RNA sample pairs of Pts. 1–4. A fixed amount of cDNA was then subjected to PCR with 25, 27 and 30 cycles, and the amplified products were quantified based on their band intensities in agarose gels. An example of such RT-PCR analysis is shown in Fig. 3 for *FGD1* and *PIM2* and the control *G3PDH*. The data for the 21 distinct transcripts are summarized in Table 2. Although it is not practical to compare the amount of PCR product among genes, the amount of a given transcript may well be compared among RNA samples. It is thus clear that expression of all of the transcripts examined, except those of *CHD4* and *FBLN1*, were higher (by more than threefold) in the tumor tissues compared to the adjacent normal tissues (see the T/N ratio column in Table 2). This strengthens the validity of the microarray data and indicates that most of the 106 genes listed in supplementary Table 2, http://www.dna-res.kazusa.or.jp/11/5/03/supplement_table/table2.html, represent genes that are highly expressed in seminomas.

3.4. *Immunohistochemical analysis of up-regulated gene products*

We also evaluated the expression of protein products in the seminoma specimens by immunohistochemistry. Figure 4 shows sections of seminomas, CIS and the adjacent normal tissues that were stained with several distinct antibodies. The antigens that were examined, namely, DNMT3A, SOX4, CCND2, ACVR1B, FGD1 and PIM2, were selected from Table 2.

As shown by the left column, most of the seminoma cells themselves were uniformly positive for immunostaining by all the antibodies tested. DNMT3A and CCND2

Figure 1. Cluster analysis of the 13 different RNA samples that formed the basis of this study. The fluorescence intensity of each of the 115 probes shown in supplementary Table 2, http://www.dna-res.kazusa.or.jp/11/5/03/supplement_table/table2.html, was processed for cluster analysis. The resulting dendrogram, which indicates the neighboring relatedness between RNA samples, is presented at the top. Pt. indicates the patient number (Pt. 10 included in this analysis is omitted from the description in the main text, since a closer examination of this mainly seminomatous testis revealed the co-existence of a minor choriocarcinoma tissue). T and N represent RNAs prepared from the tumor and adjacent normal regions of the testes, respectively. Gene symbols are shown alongside the matrix presentation. In each dot, red and green coloring represents higher and lower fluorescence intensity, respectively.

Table 2. Relative amounts of 21 transcripts as determined by semi-quantitative RT-PCR.

Gene symbol	Map	Pt.1-T	Pt.1-N	Pt.2-T	Pt.2-N	Pt.3-T	Pt.3-N	Pt.4-T	Pt.4-N	T/N ratio
AF1Q	1q21	21	4	11	1.9	22	3.3	2.8	2.1	4.8±2.1
IL6R	1q21	73	8.7	73	11	81	8.3	36	5.4	7.7±1.3
RAB25	1q21.2	98	4.8	88	35	101	3.7	104	21	13±10
KIF3C	2p23	27	4	22	2.6	25	2.8	14	3.1	7.2±1.6
DNMT3A	2p23	48	9.8	40	3.8	44	10	14	1.8	7.0±2.5
GTF3C2	2p23.3	54	20	48	10	54	21	33	2.3	5.9±4.7
E2F3	6p22	15	2.2	12	2.2	11	1.8	11	ND	>6.2±2.7
SOX4	6p22.3	74	16	60	6	64	15	4.3	1.6	5.3±2.7
OSBPL3	7p15	75	4.1	67	8.8	85	12	55	3.4	12.2±4.8
HOXA1	7p15.3	65	1.7	60	1.9	64	2.1	16	ND	>33±3.3
CCND2	12p13	67	1.7	44	15	46	6.8	44	9.9	13±14
CHD4	12p13	74	45	43	17	61	23	23	7	2.5±0.6
SLC2A3	12p13.3	56	5.8	32	4.9	35	6.6	58	7.4	7.3±1.6
FKBP4	12p13.33	86	36	60	23	62	31	47	8.9	3.0±1.3
CACNB3	12q13	70	14	51	7.1	68	12	37	3.6	7.0±2.1
ACVR1B	12q13	54	24	41	12	51	10	29	2.1	5.9±4.4
NELL2	12q13.11-q13.12	18	8.8	38	2	31	3.3	2.5	ND	>9.9±7.2
MCM5	22q13.1	65	20	55	9.4	56	12	48	5.8	5.4±1.9
FBLN1	22q13.31	78	31	80	59	87	56	65	56	1.6±0.5
FGD1	Xp11.21	87	14	58	12	70	9.2	14	4.8	5.3±1.7
PIM2	Xp11.23	77	7.1	64	5.4	63	4.9	56	19	9.6±3.9
G3PDH		163	156	163	167	144	144	167	135	1.0±0.1

See Supplementary Table 2, http://www.dna-res.kazusa.or.jp/11/5/03/supplement_table/table2.html, for the authentic names of gene symbols. The T/N ratio represents the average ± standard deviation obtained for the four patients. ND means not detected. Note that the amount of PCR product for a respective gene may well be compared between different patients, but it is not practical to compare the amount of PCR product between different genes. G3PDH was used as a reference.

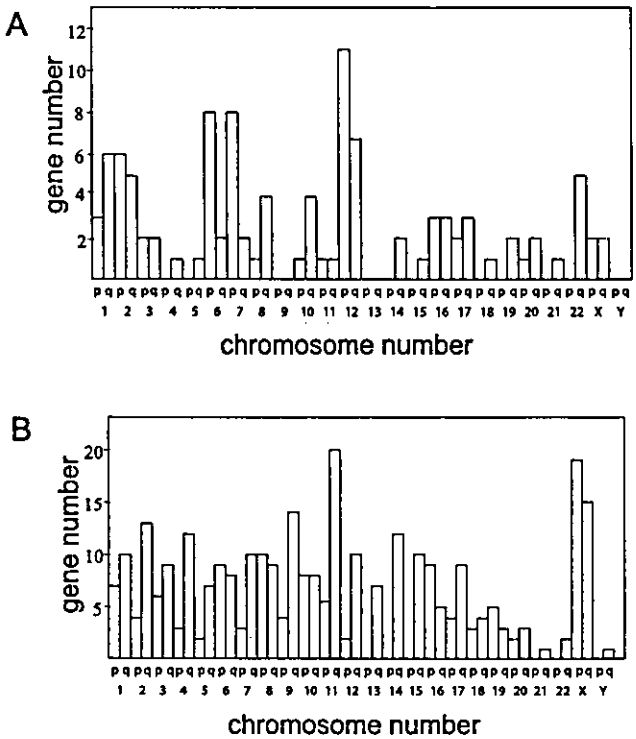

Figure 2. The number of up- and down-regulated genes that map to each chromosome. The numbers of genes that were up- and down-regulated in the seminoma samples were mapped to the short (p) and long (q) arms of each chromosome. There were 106 and 308 up- (A) and down-regulated (B) genes, respectively.

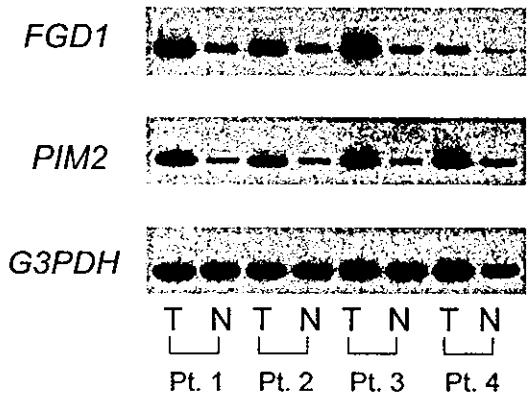

Figure 3. Semi-quantitative RT-PCR. Relative amounts of the *FGD1*, *PIM2* and *G3PDH* transcripts were compared between the tumor-derived (T) and adjacent normal tissue-derived (N) RNAs. The PCRs shown employed 25 cycles for each transcript. The amplified products were then run through agarose gels.

are known to be nuclear antigens whereas FGD1 and PIM2 are cytoplasmic/cell membrane antigens. The subcellular localization patterns of these proteins are consistent with their putative functions. Unexpectedly, however, ACVR1B, a membrane receptor, was present both in the nucleus and cytoplasm and the antibody specific for SOX4, a transcription factor, stained positively in the cytoplasm. Note that the infiltrating mononuclear cells and the endothelial cells that line the capillaries are not immunostained (arrows).

The CIS cells in the middle column were also immunos-

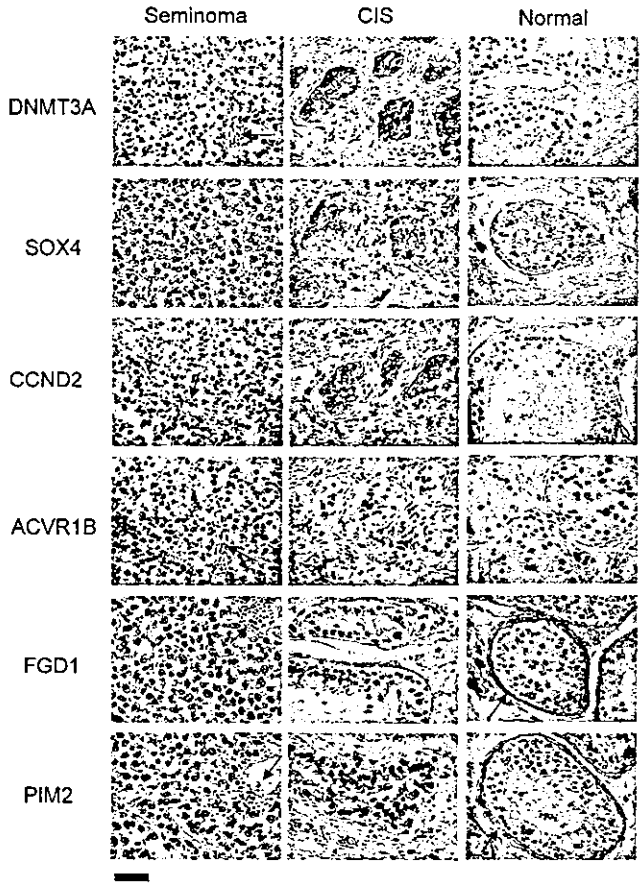

Figure 4. Immunohistochemical staining of representatives of the up-regulated proteins in the seminoma (left column), the CIS (middle column), and the adjacent normal tissues (right column). The antibodies used were specific for DNMT3A, SOX4, CCND2, ACVR1B, FGD1, and PIM2, as indicated. The arrows in the seminoma column indicate the infiltrating mononuclear cells and/or endothelial cells that line the capillaries, none of which stained positively. In the normal testes stained by anti-FGD1 and anti-PIM2, the arrows indicate the nonspecifically stained contours of the seminiferous tubules. The bar in the lowest left corner indicates the length (50 μm).

tained by each antibody. In contrast, the germ cells in the seminiferous tubules of the normal tissues adjacent to the seminomas were not immunostained at all by the antibodies (right column). An exception was DNMT3A, which stained positively but only cells at a specific stage of spermatogenesis. These cells probably correspond to the pachytene to early round spermatid stages. Thus, the results shown in Fig. 4 indicate overall that, in the case of the 6 genes selected from the 21 genes listed in Table 2, their protein expression is up-regulated in seminomas as well as in CIS cells.

3.5. Screening for down-regulated genes in seminomas

We next searched for the probes that yielded N/T ratios that exceeded 3.0 for all four of the paired RNA samples of Pts. 1–4. In total, 343 probes were extracted. Their details are shown in supplementary Table 3, http://www.dna-res.kazusa.or.jp/11/5/03/supplement_table/table3.html. The style of presentation used in supplementary Table 3, http://www.dna-res.kazusa.or.jp/11/5/03/supplement_table/table3.html, is similar to that in supplementary Table 2, http://www.dna-res.kazusa.or.jp/11/5/03/supplement_table/table2.html, except that it employs N/T ratios instead of T/N ratios. When we took into account that some genes were represented by multiple probes, the number of down-regulated gene candidates was reduced to 308. Cluster analysis using these 308 genes again resulted in the clear separation of the RNAs derived from seminoma and adjacent normal tissue (data not shown).

The number of genes that mapped on each arm of each chromosome was counted and the result is shown in Fig. 2B. The candidate down-regulated genes were distributed relatively evenly throughout the chromosomes except the X chromosome. This is in contrast to the up-regulated genes, which showed a tendency to cluster on several specific chromosomal arms as described above.

Table 3. The number of up-regulated transcripts as classified into functional groups.

Class		Number of transcripts	
(A) Functions that many kinds of cells use			
A I	Transpotation and binding proteins for ions and small molecules		13
A II	RNA processing,polymerizing,splicing and binding proteins,and enzymes		6
A III	Cell replication,histones,cyclins and allied kinases,DNA polymerases,topoisomerases,DNA modification		18
A IV	Cytoskelton and membrane proteins		4
A V	Protein synthesis co-factors,tRNA synthetases,ribosomal proteins		1
A VI	Intermediary synthesis and catabolism enzymes		3
A VII	Stress response,detoxification and cell defense proteins		2
A VIII	Protein degradation and processing,proteases		2
A IX	Transpotation and binding proteins for proteins and other macromolecules		2
		Subtotal	51
(B) Cell-cell communication			
B I	Signaling receptors,including cytokine and hormone receptors,and signaling ligands		6
B II	Intracellular signal transduction pathway molecules including kinases and signal intermediates		13
B III	Extracellular matrix proteins and cell adhesion		5
		Subtotal	24
(C) Transcription factors and other gene regulatory proteins			16
		Subtotal	16
(D) Not enough information to classify			15
		Subtotal	15
		Total	106

See Table 4 as for the details of each transcript.

4. Discussion

In the present study, we assessed the genome-wide gene expression in seminoma tissues and compared this to the expression patterns in adjacent normal tissues. This analysis revealed that 106 genes are significantly and consistently up-regulated in the seminoma tissues. Semi-quantitative RT-PCR analysis of the expression in seminoma and normal adjacent tissues of 21 of these 106 genes (Table 2) revealed that 19 of the 21 genes are indeed up-regulated in seminomas. This validates the microarray data. It is thus likely that the 106 genes that we identified reflect the alteration of gene expression that is specific to seminoma cells. Furthermore, immunohistochemical analysis of six gene products (Fig. 4) revealed strong and specific staining of tumor cells. This suggests that these proteins may be useful as molecular pathological markers of seminomas.

When we analyzed the up-regulated genes according to their location on the short and long arms of each chromosome, we found that they were not evenly distributed as several chromosomal regions seem to possess more up-regulated genes than others. Indeed, 42 of the 106 up-regulated genes are concentrated on only eight chromosomal regions such as 1q21, 2p23, 6p21-22, 7p14-15, 12p11, 12p13, 12q13-14, and 22q12-13. It has been previously reported that these chromosomes/chromosomal regions often gain chromosomal sequences in seminomas.[2] In particular, the presence of iso-chromosome 12p and the amplification of 12p-sequences are hallmarks of invasive testicular germ cell tumors.[8] Consistent with this finding is the observation that 12p contained the largest number of up-regulated genes. Thus, our gene list may be useful as a basis for the further analysis of candidate genes that are indicative of the presence of seminomas and/or are responsible for the development of seminoma.

In Table 3, the 106 up-regulated genes are categorized according to their putative functions. The gene classification used here is based on our previous reports on cDNAs/ESTs of ascidian hemocytes[19,20] and Table 4 illustrates each gene thus categorized. It is interesting to find that a number of genes were grouped into class AIII (cell and DNA replication-related), class BII (signal transducing molecules) and class C (transcription factors). Namely, 18, 13 and 16 genes belonged to classes AIII, BII and C, respectively. The up-regulation of the class AIII genes may be related to the observation that the expansion of seminoma cells is usually very rapid compared to the tumor cells in other tissues. Of these, *CCND2* is the best-studied gene in relation to testicular germ cell tumors. This gene is located on 12p13 and it is amplified and highly expressed in seminomas.[14–18] Up-regulation of genes in classes BII and C is noteworthy since these genes have the potential to become a cause of

Table 4. Up-regulated transcripts as classified into functional groups.

Class	Title	Gene Symbol
AI	fatty acid binding protein 7, brain	FABP7
AI	oxysterol binding protein-like 3	OSBPL3
AI	ATPase, H+ transporting, lysosomal 42kD, V1 subunit C, isoform 1	ATP6V1C1
AI	selenium donor protein	SPS ·
AI	prostate cancer overexpressed gene 1	POV1
AI	potassium inwardly-rectifying channel, subfamily J, member 8	KCNJ8
AI	solute carrier family 2 (facilitated glucose transporter), member 3	SLC2A3
AI	calcium channel, voltage-dependent, beta 3 subunit	CACNB3
AI	ATP-binding cassette, sub-family D (ALD), member 4	ABCD4
AI	cellular retinoic acid binding protein 1	CRABP1
AI	potassium inwardly-rectifying channel, subfamily J, inhibitor 1	KCNJN1
AI	solute carrier family 23 (nucleobase transporters), member 1	SLC23A1
AI	neuronatin	NNAT
AII	ribonucleotide reductase M2 polypeptide	RRM2
AII	U3 snoRNP-associated 55-kDa protein	U3-55K
AII	U6 snRNA-associated Sm-like protein	LSM5
AII	DEAD/H (Asp-Glu-Ala-Asp/His) box polypeptide 11 (CHL1-like helicase homolog, S. cerevisiae)	DDX11
AII	exosome component Rrp46	RRP46
AII	small nuclear ribonucleoprotein polypeptide A'	SNRPA1
AIII	ALL1-fused gene from chromosome 1q	AF1Q
AIII	DNA (cytosine-5-)-methyltransferase 3 alpha	DNMT3A
AIII	candidate mediator of the p53-dependent G2 arrest	REPRIMO
AIII	high-mobility group (nonhistone chromosomal) protein isoforms I and Y	HMGIY
AIII	H2B histone family, member A	H2BFA
AIII	H2B histone family, member G	H2BFG
AIII	H2B histone family, member J	H2BFJ
AIII	H2B histone family, member K	H2BFK
AIII	cell cycle progression 2 protein	CPR2
AIII	DNA2 DNA replication helicase 2-like (yeast)	DNA2L
AIII	antigen identified by monoclonal antibody Ki-67	MKI67
AIII	cyclin D2	CCND2
AIII	chromodomain helicase DNA binding protein 4	CHD4
AIII	nucleosome assembly protein 1-like 1	NAP1L1
AIII	cyclin F	CCNF
AIII	DNA replication factor	CDT1
AIII	MCM5 minichromosome maintenance deficient 5, cell division cycle 46 (S. cerevisiae)	MCM5
AIII	high-mobility group (nonhistone chromosomal) protein 4	HMG4
AIV	adducin 2 (beta)	ADD2
AIV	kinesin family member 3C	KIF3C
AIV	nebulin	NEB
AIV	tubulin, beta polypeptide	TUBB
AV	eukaryotic translation initiation factor 4E-like 3	EIF4EL3
AVI	putative ATPase	HSA9947
AVI	Not56 (D. melanogaster)-like protein	NOT56L
AVI	translocase of inner mitochondrial membrane 8 homolog A (yeast)	TIMM8A
AVII	defensin, beta 1	DEFB1
AVII	metallothionein 1H	MT1H
AVIII	matrix metalloproteinase 12 (macrophage elastase)	MMP12
AVIII	phorbol-12-myristate-13-acetate-induced protein 1	PMAIP1
AIX	sorting nexin 10	SNX10
AIX	Bicaudal D homolog 1 (Drosophila)	BICD1

Class	Title	Gene Symbol
BI	interleukin 6 receptor	IL6R
BI	sema domain, transmembrane domain (TM), and cytoplasmic domain, (semaphorin) 6A	SEMA6A
BI	low density lipoprotein receptor-related protein 6	LRP6
BI	activin A receptor, type IB	ACVR1B
BI	peptide YY	PYY
BI	opioid growth factor receptor	OGFR
BII	protein kinase, AMP-activated, beta 2 non-catalytic subunit	PRKAB2
BII	SHC (Src homology 2 domain containing) transforming protein 1	SHC1
BII	RAB25, member RAS oncogene family	RAB25
BII	tumor-associated calcium signal transducer 1	TACSTD1
BII	zinc finger protein RINZF	RINZF
BII	FK506 binding protein 4 (59kD)	FKBP4
BII	mitogen-activated protein kinase kinase kinase 12	MAP3K12
BII	dual-specificity tyrosine-(Y)-phosphorylation regulated kinase 2	DYRK2
BII	huntingtin interacting protein 12	HIP12
BII	JAK binding protein	SSI-1
BII	ankyrin repeat domain 3	ANKRD3
BII	faciogenital dysplasia (Aarskog-Scott syndrome)	FGD1
BII	pim-2 oncogene	PIM2
BIII	integral membrane protein 3	ITM3
BIII	NEL-like 2 (chicken)	NELL2
BIII	claudin 6	CLDN6
BIII	cadherin 3, type 1, P-cadherin (placental)	CDH3
BIII	fibulin 1	FBLN1
C	general transcription factor IIIC, polypeptide 2 (beta subunit, 110kD)	GTF3C2
C	zinc finger protein 142 (clone pHZ-49)	ZNF142
C	KRAB-zinc finger protein SZF1-1	SZF1
C	E2F transcription factor 3	E2F3
C	SRY (sex determining region Y)-box 4	SOX4
C	homeo box A1	HOXA1
C	nuclear respiratory factor 1	NRF1
C	homeo box HB9	HLXB9
C	fibrinogen silencer binding protein	FSBP
C	forkhead box H1	FOXH1
C	undifferentiated embryonic cell transcription factor 1	UTF1
C	early development regulator 1 (polyhomeotic 1 homolog)	EDR1
C	T-cell leukemia/lymphoma 1B	TCL1B
C	tumor protein p53 (Li-Fraumeni syndrome)	TP53
C	zinc finger protein 144 (Mel-18)	ZNF144
C	zinc finger protein 278	ZNF278
D	hypothetical protein FLJ10684	FLJ10684
D	hypothetical protein FLJ12457	FLJ12457
D	hypothetical protein FLJ12505	FLJ12505
D	KIAA1155 protein	KIAA1155
D	hypothetical protein FLJ20059	FLJ20059
D	hypothetical protein FLJ20627	FLJ20627
D	KIAA0363 protein	KIAA0363
D	KIAA1886 protein	DKFZP761I2123
D	DKFZP564D206 protein	DKFZP564D206
D	hypothetical protein FLJ10339	FLJ10339
D	putative protein similar to nessy (Drosophila)	C3F
D	hypothetical protein FLJ10665	FLJ10665
D	hypothetical protein FLJ22865	FLJ22865
D	hypothetical protein FLJ21603	FLJ21603
D	KIAA0767 protein	KIAA0767

As for the details of classes, see Table 3.

further alteration in gene expression. If a gain of chromosomal material hits and induces one of these genes, then its elevated expression might lead to changes in the expression of other genes. Therefore, the list of 106 genes might include both genes with direct effects caused by a gain of chromosomal material and genes affected by the up-regulation of the genes in classes BII and C. Of these, transcription factors such as E2F3, HOXA1 and SOX4 have been reported to be somehow involved in cell transformation. E2F3 is a cell cycle-related protein.[21] In mammary tumors, HOXA1 is highly expressed[22] and its forced expression can transform normal mammary epithelial cells into tumor cells.[23] In mice, the *SOX4* gene is a common integration site (*Evi16*) in retrovirus-induced, murine leukemia/lymphoma.[24] Another interesting feature seen from Table 3 is that the number of genes classified as AVIII (protein degradation) and BIII (extracellular matrix and cell adhesion protein) is relatively low (2 and 5, respectively). This point, however, remains to be examined in more detail in the future, since one half of the patients selected in this study suffered from metastasis and the other half did not.

The microarray analysis also revealed 308 candidate genes that are down-regulated in seminomas compared to adjacent normal tissues. The chromosomal distribution pattern of these genes differs from that of the up-regulated genes (compare Figs. 2A and 2B). While 12p has 11 up-regulated genes, it has only 2 down-regulated genes. In contrast, 4q has 12 down-regulated genes but only 1 up-regulated gene, while 11q has 20 down-

regulated genes yet only 1 up-regulated gene. This pattern reflects previous observations that 4q and 11q are frequent sites of chromosomal deletion in seminoma.[2] Another factor that might contribute to the down-regulation of gene expression would be the status of promoter methylation of genes. In this respect, the up-regulation of *DNMT3A* as described above is worth mentioning since it is involved in the *de novo* methylation of DNA during embryonic development,[25,26] and its protein expression was detected in seminoma cells as well as spermatocytes/round spermatids in normal testis (Fig. 4). Therefore, DNMT3A might function in the methylation of gene promotors in the tumor cells, although the genome derived from seminoma is reported to be in a hypomethylated status in general.[27] It should be noted, however, that the down-regulated transcripts may merely reflect the lack of some specific cell types in the seminoma. For example, *transition protein 1* and *protamine 1* are included in supplementary Table 3, http://www.dna-res.kazusa.or.jp/11/5/03/supplement_table/table3.html, which lists the down-regulated genes in seminoma. These two genes are expressed specifically in the haploid spermatids in the normal testis and the seminoma tissues are obviously devoid of such normally differentiated cells.

Recently, similar genome-wide surveys of gene expression in seminomas have been conducted independently by two other laboratories.[28,29] These studies identified 347 and 1,518 transcripts that are up-regulated in seminoma, respectively. When we compared our list of 106 up-regulated genes with theirs, we found to our surprise that only 13 and 41 of our genes were present among the 347 and 1,518 genes, respectively. Furthermore, only the transcripts of 9 genes, namely *IL6R*, *DNMT3A*, *KIF3C*, *SOX4*, *POV1*, *CCND2*, *ABCD4*, *CDH3* and *MCM5*, were found to be up-regulated in all three studies. This means that a significant portion of our gene list differs from theirs. Although the exact reason for this difference is not clear, one reason may be the control samples that were used. In the study of Ref. 28, one RNA sample from normal testis (Clontech) was used as a control, whereas, in the study of Ref. 29, 14 samples of normal testes as well as 17 somatic cell lines were used as controls. In the present study, however, we employed four normal testis tissues as controls which were localized adjacent to the tumor regions. A second factor may be that different oligonucleotide (our study) and cDNA arrays (Refs. 28 and 29) were used in the different studies. A third factor may be the method of gene extraction used. In Ref. 28, genes were selected whose expression was higher in more than half of informative seminoma samples compared to normal RNA, whereas in the study of Ref. 29, a method of significance analysis of microarrays[30] was used to extract the up-regulated genes. In our study, we picked up the transcripts whose elevated expression was detected in all four seminoma samples compared to the same patient's normal tissues.

In conclusion, whatever the reason is for the difference between our results and those of previous studies, one advantage of our study would be that we could remarkably reduce the number of genes of interest. A number of 106 as the up-regulated genes is not too large to start analyzing the functions of individual genes. Secondly, we could map 42 of the 106 genes to 1q21, 2p23, 6p21-22, 7p14-15, 12p11, 12p13, 12q13-14 and 22q12-13. These regions are included in those which were reported to be the frequent sites of gain of chromosomal material by a method of comparative genomic hybridization.[2] Thus, these 42 genes could be of particular interest for further study. Finally, functional classification of 106 up-regulated genes revealed unique features associated with seminoma.

Acknowledgements: This work was supported in part by research grants from the Ministry of Education, Science, Sports, Culture and Technology, Japan. M.S. is a member in the 21st Century COE program "Center for Innovative Therapeutic Development Towards the Conquest of Signal Transduction Diseases" that is headed by K. Sugamura at Tohoku University. We would like to express our thanks to M. Nishigaki for assistance with the microarray analysis and to M. Kuji for secretarial assistance.

References

1. Chaganti, R. S. K. and Houldsworth, J. 2000, Genetics and biology of adult human male germ cell tumors, *Cancer Res.*, **60**, 1475–1482.
2. Skotheim, R. I. and Lothe, R. A. 2003, The testicular germ cell tumor genome, *APMIS*, **111**, 136–151.
3. Oosterhuis, J. W., Castedo, S. M., de Jong, B. et al. 1989, Ploidy of primary germ cell tumors of the testis. Pathogenetic and clinical relevance, *Lab. Invest.*, **60**, 14–21.
4. de Graaff, W. E., Oosterhuis, J. W., de Jong, B. et al. 1992, Ploidy of testicular carcinoma in situ, *Lab. Invest.*, **66**, 166–168.
5. El-Naggar, A. K., Ro, J. Y., McLemore, D. et al. 1992, DNA ploidy in testicular germ cell neoplasms, *Am. J. Pathol.*, **16**, 611–618.
6. Atkin, N. B. and Baker, M. C. 1982, Specific chromosome change, i(12p), in testicular tumours? *The Lancet*, **2**, 1349.
7. van Echten, J., Oosterhuis, J. W., Looijenga, L. H. J. et al. 1995, No recurrent structural abnormalities apart from i(12p) in primary germ cell tumors of the adult testis, *Genes, Chrom. Cancer*, **14**, 133–144.
8. Looijenga, L. H. J., Zafarana, G., Grygalewicz, B. et al. 2003, Role of gain of 12p in germ cell tumor development, *APMIS*, **111**, 161–173.
9. Rodriguez, E., Houldsworth, J., Reuter, V. E. et al. 1993, Molecular cytogenetic analysis of i(12p)-negative human male germ cell tumors, *Genes, Chrom. Cancer*, **8**, 230–236.
10. Suijkerbuijk, R. F., Sinke, R. J., Meloni, A. M. et al. 1993,